MODIFIED CORNER REFLECTOR ANTENNA FED BY A PRINTED DIPOLE ON A QUARTER CYLINDRICAL SUBSTRATE

BY

EQAB FAHED A. KHLEIF

A Thesis Presented to the

DEANSHIP OF GRADUATE STUDIES

KING FAHD UNIVERSITY OF PETROLEUM & MINERALS

DHAHRAN, SAUDI ARABIA

In Partial Fulfillment of the

Requirements for the Degree of

MASTER OF SCIENCE

In

ELECTRICAL ENGINEERING

DECEMBER 2013

KING FAHD UNIVERSITY OF PETROLEUM & MINERALS
DHAHRAN 31261, SAUDI ARABIA

DEANSHIP OF GRADUATE STUDIES

This thesis, written by **EQAB F. KHLEIF** under the direction of his thesis adviser and approved by his thesis committee, has been presented to and accepted by the Dean of Graduate Studies, in partial fulfillment of the requirements for the degree of **MASTER OF SCIENCE IN ELECTRICAL ENGINEERING**

.

Thesis Committee

H. A. Ragheb
Dr. Hassan A. Ragheb (Adviser)

(Co-adviser)

Dr. Esam Hassan (Member)

Dr. Sheikh Sharif Iqbal (Member)

(Member)

Dr. Ali Al Sheikhi
Department Chairman

Dr. Salam A. Zummo
Dean of Graduate Studies

17/12/13
Date

عمادة الدراسات العليا
DEANSHIP OF GRADUATE STUDIES

To my parents, my wife, and my kids

ACKNOWLEDGMENTS

First of all I would like to thank my Thesis adviser Prof. Hassan Ragheb for his unlimited patience, support, and advice during my work. Also thanks to my Thesis committee members Prof. Esam Hassan and Prof. Sharif Iqbal, who contributed useful feedback throughout this research, specially in the part related to the fabrications and measurements. I would like to express my deep gratitude to all those who gave me the possibility to complete this thesis. In exception of my work efforts, there have been several people contributing to the quality of this study. Many thanks to KFUPM lab technicians who helped in the fabrication and testing of the antenna. Finally a special thanks to my parents and my wife for giving me encouragement and strength to achieve my goals. Without their support, this effort would not have been possible.

TABLE OF CONTENTS

LIST OF TABLES

LIST OF FIGURES

LIST OF ABBREVIATIONS

CR Corner Reflector

CCR Cylindrical corner reflector

SCR Square Corner reflector

WiFi Wireless Fidelity

HFSS high Frequency Structures Simulator

VSWR Voltage Standing Wave Ratio

HPBW Half Power Beam Width

3GPP 3rd generation Partnership Project

SNR Signal To Noise ratio

IP TV Internet Protocol TV

SLS Side Lobe Suppression

MIC Microwaves Integrated Circuits

RL Return Loss

PA Printed Antenna

RFID radio Frequency Identity

PDA Printed Dipole Antenna

MSA Microstrip Antenna

GPS Global Positioning system

GSM Global System For Mobile Communication

WLAN Wireless Local Area Network

WG Wave Guides

MIMO Multiple Input Multiple Output

FEM Finite Element Method

LTE Long Term Evolution

VNA vector Network Analyzer

PCB Printed Circuit Board

dBi Gain in Decibels with reference to isotropic radiator

BS Base Station

FSLA First Side Lobe Attenuation

ISM Industrial, Scientific , And Medical

THESIS ABSTRACT

NAME: Eqab F. Khleif

TITLE OF STUDY: Modified Corner Reflector Antenna fed by a Printed Dipole on a Quarter Cylindrical Substrate

MAJOR FIELD: Electrical Engineering

DATE OF DEGREE: December 2013

Corner reflector (CR) fed by printed dipole antenna is an emerging research field and expected to play an important role in the wireless communication industry. In particular, for applications that requires simple, low cost, high gain, and super directive antennas. In this Thesis a printed strip dipole is used as a feed for the conventional cylindrical corner reflector (CCR). The proposed antenna is rigid, mechanically stable, and overcomes disadvantages associated with using the wire dipole as feed. It also provides a variety of printed antenna designs to replace the conventional wire dipole used for CR and CCR, hence improves the antenna performance. It can also be used to improve the performance of 802.11 WiFi 2.4GHz devices, where omni directional antenna is used in such applications. The designed antenna is optimized using professional software to demonstrate the op-

timal antenna characteristics. The simulation of the first prototype has provided an impedance bandwidth of 310 MHz at VSWR=2, gain of 12.4dB, and a HPBW of 67^o *which is suitable for sector zone applications. The antenna is fabricated and experimentally tested. Experimental and simulated results are found in good agreement. The second prototype with passive dipole strips is investigated to provide a broadband characteristics that covers additional 3GPP frequency bands for wireless broadband communications. We were able to demonstrate a good performance antenna for 2.1G, 2.3G, 2.4G, 2.6G frequency bands were covered with a very good VSWR below 2 and with 1.3GHz impedance bandwidth. This antenna is simply constructed by adding two parasitic elements longitudinal to the main radiator. The resulting design is still simple and low cost.*

خلاصة أطروحة

الاسم : عقاب فهد خليف

عنوان الاطروحه : عاكس زاوية اسطواني مغذى عن طريق هوائي شريطي مطبوع على قاعدة اسطوانية عازلة

التخصص العام : الهندسه الكهربائية

التاريخ : تشرين الثاني ٢٠١٣

في هذه الاطروحة سيتم عرض هوائي جديد تم تصميمه باستخدام الهوائيات الشريطية المطبوعة وبالاخص تلك الثنائية القطب المستخدمة لتغذيه الهوائيات العاكسة ذات الزاوية القائمة. هذا النوع من العاكسات ذات الزاويه القائمه يستخدم عادة لزيادة توجيه الاشارات الكهرومغناطيسية، عادة تتم تغذيته هذا النوع من الهوائيات عن طريق هوائي سلكي ثنائي القطب. ان انظمة الاتصالات المعاصرة كالشبكات اللاسلكيه المحلية $(WLANorWiFi)$ اصبحت تتطلب هوائيات ذات قدرة توجيه عالية وكذلك عرض حزمة ترددات كبير و هذا بعكس تلك الهوائيات المستخدمة حاليا و التي لا توفر اي قدره على التوجيه وتقوم بالبث في جميع الاتجاهات بالاضافة الى عرض حزمه ترددات ضيق. هذا النوع من الهوائيات قد ينتج عنه الكثير من التداخل في الترددات كنتيجة لكثافه الاستخدام و البث في كل الاتجاهات و من هنا تاتي الحاجة الى هوائيات ذات قدرة توجيه عالية.

الهوائي المقترح يعمل على حل هذه المشكة في الترددات الخاصة والمستخدمة في تطبيقات الشبكات المحليه $WLAN-ISM2.4GHz$ و قد تم تعديل الهوائي المقترح كذلك للعمل على ترددات اضافيه عديدة والمستخدمة في شبكات الجيل الثالث والرابع . هذا الهوائي الجديد هو بسيط من حيث التصميم و مكون من ثلاث صفائح نحاسه عاكسة الاولى و الثانيه مستوية وعلى شكل زاوية قائمة والثالثة عبارة عن جزء من

اسطوانة قائمة . تتم تغذيتة عن طريق هوائي شريطي ثنائي و مطبوع على قاعده عازلة ذات شكل اسطواني. هذا النوع من العاكسات له تاثير كبير على قدره التوجية بحيث اصبح بالامكان الحصول على هوائي ذات مزايا متعدده و مناسب للعديد من التطبيقات. لقد تم تصميم و محاكاة و تنفيذ نموذج اولي للهوائي المقترح باستخدام برنامج المحاكاة $(HFSS)$ وكذلك تمت تجربة الهوائي في مختبر خاص للتأكد من خصائصه الترددية و الاشعاعيه بالاضافة الى كفائة الاشعاع و قدرته على التوجيه. تم تحليل نتائج المحاكاة للنموذج الاولي واللتي اظهرت قدرة توجية عالية مساوية ل $(12.4dBi)$ وكذلك سعة حزمة ترددية $(310MHz)$ وذات نطاق اشعاعي $HPBW = 75^o$ وبعد تعديل التصميم للحصول على عرض حزمة ترددات اكبر كانت نتيجة المحاكاة حوالي $(1.3GHz)$ ، واصبح بالامكان استخدام الهوائي المقترح في تطبيقات الجيل الثالث والرابع للاتصالات المتنقلة بنفس الكفاءة . لقد اظهرت النتائج العمليه توافق كبير مع تلك النتائج التي حصلنا عليها من الحسابات النظرية و كذلك الناتجة من المحاكاة عند معظم الترددات التي اجريت عندها القياسات.

CHAPTER 1

MOTIVATION AND THESIS STRUCTURE

1.1 Thesis Motivation

Personal communication has evolved very rapidly in the recent few years, almost every person carries at least one device that has one or more antenna to communicate with wireless networks like 2G, 3G, 4G, or WiFi. In this Thesis, a 2.4Ghz WiFi novel directional antenna is proposed. The antenna is build based on cylindrical corner reflector, supported by a cylindrical surface to achieve high gain and super directive radiation pattern[1]. The conventional CCR uses a wire dipole as a feed element, which makes the CCR less robust and reliable antenna. The new design suggests using a new feed element which is a printed dipole antenna mounted on a quarter cylindrical substrate, which gives a broad side linearly polarized radiation pattern. The printed antennas provides a wide range of design

options. The main purpose is to provide an alternative solution for omni directional antennas and present a new concept of directional integrated antennas for WiFi use. This antenna is robust and it overcomes the mechanical stability issues experienced using traditional corner reflectors with wire dipole radiating element. This antenna is designed to work on the WiFi 2.4Ghz band, which enabled a new field for designing directional integrated antenna for the use in WiFi Access Points sectorized coverage.

The need for WiFi directional antenna became very crucial requirement in design of WiFi coverage and capacity. The directional antenna enhances the coverage in certain direction and enable reaching of more customer. SNR will be enhanced which in its turn increases the capacity as per Shannon theorem. The user throughput will increase and so the user experience. Furthermore it will be possible to enable new services over WiFi network like the IPTV which requires high performance WiFi network and high data throughput. Also the directional antenna enables the reuse of the spectrum resources more often. The heavy usage of WiFi hot-spots requires new techniques for interference mitigation. A key solution is using directional WiFi antenna rather than transmitting in all directions. By adding two parasitic elements along the main dipole, the antenna bandwidth was broaden. The BW covers new 3GPP frequency bands besides the ISM 2.4GHz band, that allowed the proposed antenna to be good candidate in third and forth generations Mobile base station applications.

1.2 Thesis Objective

The main contribution of this thesis is combining the CCR proposed by [1], with the printed strip dipoles designed and found in literature [2] [3]. The resulting structure Fig.1.1 exhibits a high gain and super directive linearly polarized(V polarization) antenna that is simulated, fabricated and tested. Toward the final antenna design, 4 models has been designed, simulated, and tested:

- Design of printed strip dipole on a planar substrate.
- Design of printed Strip Dipoles on a cylindrical substrate.
- Adding the CCR to the above step 2
- Adding the two parasitic elements to broaden the antenna bandwidth.

1.2.1 Remodeling and Assumptions

The CR and CCR are well studied in literature, but using the wire dipole as feed system. To be able to use the theory of CR, we have to convert our proposed design to a problem that can be approximated by the CCR with wire dipole feed. below are some assumptions that are applied to the proposed antenna to be able to use the background for CR/CCR

- To simplify the analysis of the proposed antenna, the printed dipole and the cylindrical substrate are replaced by an equivalent cylindrical dipole feed, analogous to the work done by T. Faton [4]. The structure is then analyzed like any other corner reflector fed by a dipole antenna. This assumption is

valid for thin substrates and for narrow strips, in our case the cylindrical equivalence will be $a = 0.25W$.

- In the analysis of the CCR with printed dipole feed, we have used the Image Theory and Uniform Circular Array Theory [5][6][1][7][8] to compute the resulting antenna radiation pattern.

- The Image theory suggest that if the reflecting plates are infinite in length, and with infinite conductivity, then we can replace the conducting plates with dipole images, equally-spaced and form a uniform circular array, with same current amplitude but with successive phase difference of 180^o.

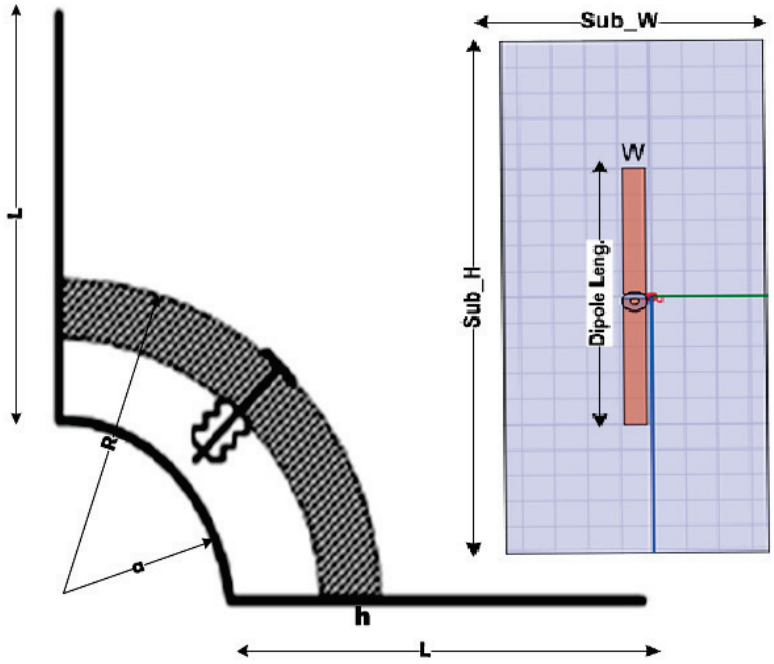

Figure 1.1: Suggested Modified CCR prototype

1.2.2 Design Optimization Techniques

The side lobe suppression SLS suggested by [9] is going to be implemented. SLS is a very important step towards providing highly directive antenna by preventing or reducing the energy transmission in a direction other than the intended azimuth. Reception from the side lobe direction causes an interference to the receiver and ambiguity in the data and information recovery. The side lobe suppression is a common problem in the corner reflector antennas due to the fact that the reflecting plates are not infinite in extent as required by the image theory. The following techniques are going to be used to reduce the side lobe level:

- Metallic scatters :

  Placed in the aperture of the CR, two metallic strips at specific position and with specific width [9].

- Triple CR [10]

  The conventional CR is modified by adding two more plates as described by Mathew [10]. The performance of the antennas was enhanced in the H plane.

- Adding Parasitic elements for BW increase

  Addition of parasitic elements is intended to increase the operating bandwidth of the antenna.

1.3 Thesis Organization

The Thesis consists of 6 chapters, the first chapter is about the thesis motivation and objectives, the second one, introduces some important aspects of antenna theory needed in this work. Literature review is introduced in chapter three where published work in the field of CR, CCR, and printed dipole antenna is included. Chapter 4 is devoted to the design of the CCR, and the printed dipole antenna. Chapter five includes the simulation results, fabrication procedure of the prototype and the lab test results are discussed. Finally; Conclusions, future work, and recommendations are included in last chapter.

CHAPTER 2

ANTENNA THEORY

2.1 History of Antenna Technology

The theoretical foundations for antennas starts from Maxwells equations. James Clark Maxwell in 1864 presented his first results, which showed that light and electromagnetic waves are similar, and electromagnetic disturbances both can be explained by waves traveling at the same speed. He unified the theories of electricity and magnetism through what is later called Maxwell's Equations [11]. In 1886 Heinrich Hertz verified the above and discovered that the electrical disturbances or a spark caused by a $\lambda/2$ dipole gap, can be detected at far distance (around 20m) with a secondary circuit like a loop antenna of proper dimensions for resonance and containing an air gap for sparks to occur [11]. After that and mainly in 1901, Guglielmo Marconi built a microwave parabolic cylinder at a wavelength of 25 cm for his original code transmission and worked at longer wavelengths for improved communication range. Marconi is considered as the father of amateur

radio. Antenna developments in the early years were limited by the availability signal generators. About 1920 resonant length antennas were possible after the De Forest triode tube was used to produce continuous wave signals up to 1MHz. Just before World War II, microwave (about 1 GHz) klystron and magnetron signal generators were developed along with hollow pipe waveguides. During the war an intensive development effort primarily detected toward radar, encouraged the development of many modern antenna types, such as large reflectors, horns, lenses, and waveguide slot arrays [11]. Later and in 1950's a breakthrough in antenna evolution occurred when it was possible to realize antennas with high bandwidth approaching 40:1, this was referred to as frequency independent antennas. This was possible due to the changed in geometry of the antenna from linear dimensions to dimensions that are defined by angles.

After that and between 1960's and 1980's, the modern antenna technology was driven by advancement on the computation capabilities of computers. Numerical methods and simulations using computers has emerged and enabled faster and more accurate analysis of antennas with different structures and geometries. Recently and in 1970's the microstrip patch antennas was developed. This radiating element is used intensively as feed element in many applications. It can be integrated with active and passive components of the MIC, and also flush mounted on any non planar structure, due to its conformability property.

2.2 Introduction to Antennas

Wireless communications are rapidly developing and driven by new applications demanding high bandwidth and need for high interference rejection, which imposes new challenge and high performance expectations to antenna system designers. Antennas are metallic structures designed for transmitting and receiving electromagnetic energy. An antenna acts as a transitional structure between the guiding device (e.g. waveguide, transmission line) and the free space. The official IEEE definition of an antenna is given by Stutzman and Thiele [12]:" That part of a transmitting or receiving system that is designed to radiate or receive electromagnetic waves". Antenna is a reciprocal device. That is a very importance property, since it will be used for transmitting and receiving of electromagnetic waves at the same time without the need for extra hardware. To understand how an antenna radiates, explained by Balanis [13]. A conducting wire radiates mainly because of time-varying current or an acceleration (or deceleration) of charge. If there is no motion of charges in a wire, no radiation takes place, since no flow of current occurs. Radiation will not occur even if charges are moving with uniform velocity along a straight wire. However, charges moving with uniform velocity along a curved or bent wire will produce radiation. If the charge is oscillating with time, then radiation occurs even along a straight wire[13].

When a sinusoidal voltage is applied across the transmission line, an electric field is created which is sinusoidal in nature and this results in the creation of electric lines of force which are tangential to the electric field, this is shown in the Fig 2.1.

Antennas in literature were found in variety of forms and shapes , depending on

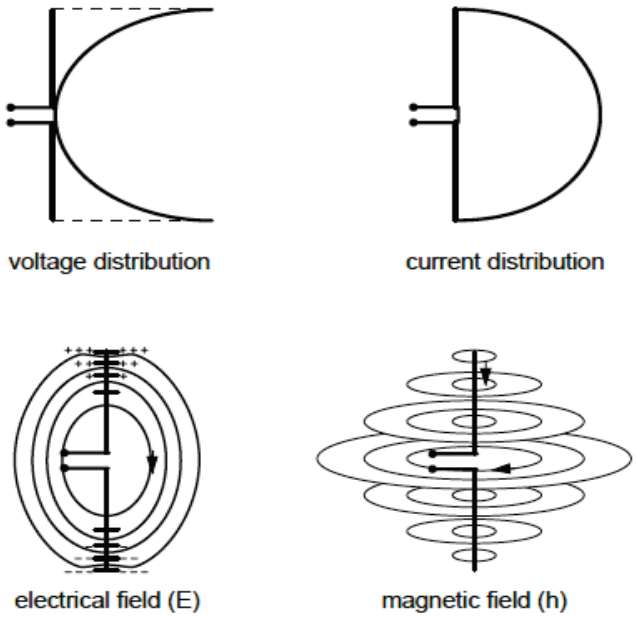

Figure 2.1: Dipole radiation due to time varying current

the application, below are main categories of antennas:

- Aperture Antennas like Horn and Wave-guides.
- Reflector antennas: corner reflectors and parabolic reflector.
- Printed Antenna like microstrip patch, and printed dipole.
- Array Antenna like the Yagi-Uda and Aperture arrays.
- Wire Antenna like dipoles and loop antennas.
- Lens Antenna.

The first and second types are referred to as aperture type structures. The high gain antennas are evolved from above types and can be one of the following :

- Reflector antennas: corner, parabolic.
- Aperture Antennas like Horn and Wave-guides.
- Microstrip array.
- Phased arrays.
- Helix

Wireless system requires high directive antenna in order to cover the desirable area and reach critical customer location, while rejecting the noise and interference. To achieve this objective, reflectors and arrays are used always for better directivity and higher gain. Reflector antennas, in one form or another, have been in use since the discovery of electromagnetic wave propagation in 1888 by Hertz. Reflectors were wildly used to modify the radiation pattern of a radiating element, by placing a plane sheet large enough at the back of the antenna to reflect the backward radiated fields as per experiment done by Brown 1937. The development of reflector antennas was supported by the applications that require high gains like: radar, deep space communication, microwave point to point system, and satellite tracking systems. The reflector antenna takes different forms based on application, the most popular forms: planar reflector, corner reflector and curved (parabolic)reflector antennas.

The 90^o aperture corner reflector antenna was modified as shown in Fig.3.4, to be mounted on the quarter cylindrical substrate, and excited by a strip printed

dipole. The reflecting sheets can be fixed in various aperture angle , it can be any sub multiple of 180^o (π/N), and the most common is the 90^o type. Ordinary corner reflector antenna used for VHF/UHF broadcast, suffers from mechanical strength due to the feed supporting system. Also wind loading might affect the location of the feed which could degrade the antenna performance. The new design should be rigid enough to avoid any mechanical displacement of the feed, the suggested feed is a printed dipole on a cylindrical substrate, and that will not degrade antenna performance. The cylindrical substrate has an influence on the resonance frequency based on the cylinder radius and reflecting sheets dimensions. In this complex structure, the reflector works as parasitic element that re radiates the impinged radiations either from or going to the radiating element, into free space, accordingly it has a direct relationship with the antenna gain. The printed strip dipoles are going to be used as the feed for the CCR to be able to use the variety of advantages that printed antenna offers. Printed dipoles are very popular due to ease fabrication, low profile,low costs and conformable to non-planar structures.

2.3 Antenna Parameters And Figure of Merits

The performance of an antenna can be measured by investigating a number of characteristics. The antenna designers are balancing between these parameters to fit certain constraint, there is no one design satisfies all parameters, but we always look for optimal one. Below are some of the important concepts in the analysis of antenna performance.

2.3.1 Antenna Input Impedance

The antenna is seen as an interface between the free space with impedance of $\eta = 120\pi$ and the device transmitter circuitry connected through the transmission line of $Z_o = 50\Omega$. Therefore it has some properties based on circuit theory like the input resistance, return loss, VSWR, some other properties like the radiation pattern, gain, polarization, are seen from EM theory point of view.

The input impedance is very important figure of merit for an antenna. It qualifies the antenna to be used in specific application. The input impedance of an antenna is essentially made of three components, as shown in Fig 2.2. These three main

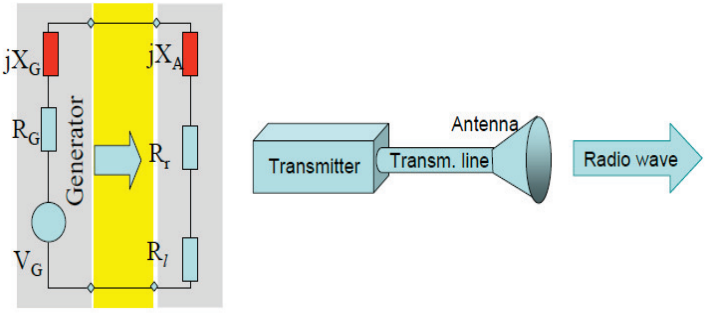

Figure 2.2: Antenna Input impedance seen from circuit theory

components are interpreted as below:

- jX_A : represents the energy stored in the H and E near field components. It must be mitigated by proper matching and optimum antenna dimensions, this is not a desirable component.

- R_r : represents the energy radiated as an electromagnetic fields (H and E) in space and forms the far field components. This is to be maximized by perfect matching to the transmission line feeding the antenna. Antenna

efficiency is a measure of energy transfer represented by this component.

- R_l : represents the loss of energy which is transformed as heat in the antenna material, this is to be minimized for perfect antenna radiation efficiency.

The Radiation resistance of the half wave dipole antenna is of a main concern, since it is directly affects the radiation patterns and gain of the antenna. Antenna theory mainly concerns about the radiation resistance and the methods for finding closed form expression for this parameter for a given antenna. Next, is one way of finding the radiation resistance. Using the Poynting Vector theorem, which represents the density of energy flow out of the enclosing surface, the average power density is normally a complex term and given by:

$$\mathbf{S} = \mathbf{S}_r + j\mathbf{S}_i \tag{2.1}$$

$$\mathbf{S}_r = \frac{1}{2} Re[\mathbf{E} \times \mathbf{H^*}] \tag{2.2}$$

The radiated power is then given by integration of the closed surface:

$$W = \oint_s \mathbf{S}_r \cdot \mathbf{ds} \tag{2.3}$$

the radiated energy is related to the radiation resistance via the following formula :

$$R_{rad} = \frac{radiated\ energy}{normalized\ current} = 2\frac{W_{rad}}{I^2} \tag{2.4}$$

Since we already know the electric and magnetic filed expression at far field generated by half wave dipole, we can easily find the radiated power , and integrate it over the surface to get the radiated energy needed to find the radiation resistance. The electric and magnetic fields of the dipole are :

$$E_\theta = j\eta \frac{I_o}{2\pi r} e^{-jkr} [\frac{cos(\frac{kl}{2} cos(\theta)) - cos(\frac{kl}{2})}{sin(\theta} \tag{2.5}$$

$$H_\phi = j \frac{I_o}{2\pi r} e^{-jkr} [\frac{cos(\frac{kl}{2} cos(\theta)) - cos(\frac{kl}{2})}{sin(\theta} \tag{2.6}$$

substituting Eq.2.5 and Eq.2.6 into Eq.2.2:

$$P_r(r, \theta, \phi) = \frac{1}{2} \eta (\frac{I_o}{2\pi r})^2 [\frac{cos(\frac{kl}{2} cos(\theta)) - cos(\frac{kl}{2})}{sin(\theta)}] \tag{2.7}$$

substituting Eq.2.7 in Eq.2.3:

$$W_{rad} = \int_0^{2\pi} d\phi \int_0^{\pi} d\theta r^2 sin\theta P_r \tag{2.8}$$

Performing the integration for half wavelength dipole, and using equations above; we can find that the radiation resistance for the half wave dipole as $R_{rad} = 73\Omega$ [13].

Another way of finding the input impedance of the antenna is through simulations. HFSS electromagnetic solvers is used in this case to study the input impedance behavior for CCR antenna and how it is affected by varying the antenna to vertex

distance. The input resistance and reactance of dipole antenna are plotted in Fig.2.4 and Fig.2.3. The real and imaginary parts of the input impedance are simulated at different values of "a" which is the radius of the reflecting cylindrical surface.

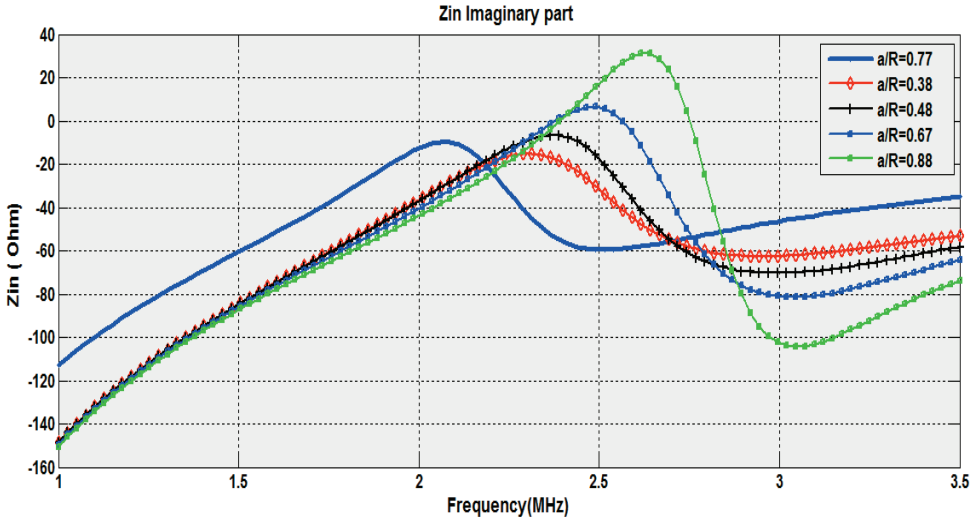

Figure 2.3: Input impedance at different "a/R" values -imaginary part

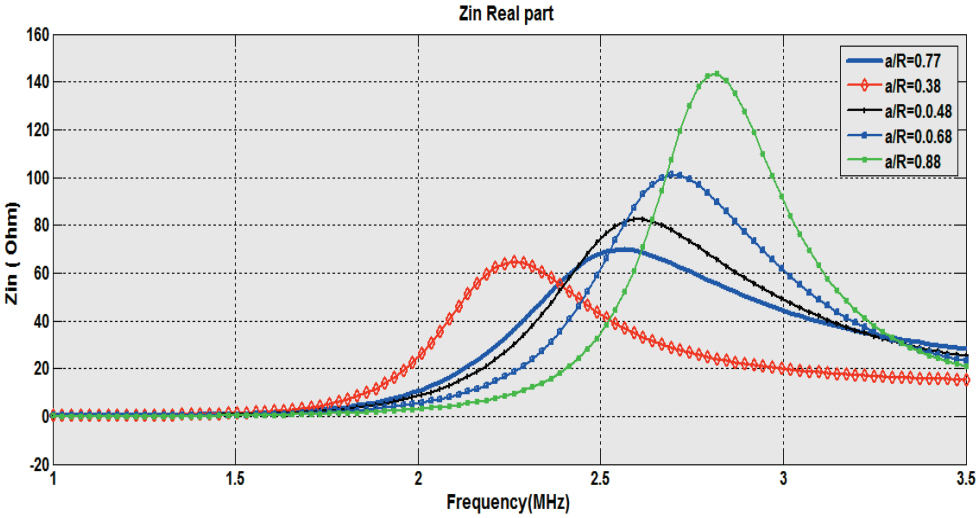

Figure 2.4: Input impedance at different "a/R" values -real part

At the designed frequency 2.4GHz, the real part must be 50Ω and imaginary part

is zero. These values can be achieved at a/R equal to 0.067. Later on these values are used in simulation and implementation of the proposed antenna prototype.

2.3.2 Radiation Efficiency

Radiation efficiency is defined by IEEE as: ratio of total power radiate by an antenna to the net power accepted by the antenna from the connected transmitter [14]. As per Fig.2.2, the antenna radiation efficiency can be mathematically given by :

$$E = \frac{P_{radiated}}{P_{accepted}} = \frac{R_r I^2}{(R_L + R_r)I^2} = \frac{R_r}{(R_L + R_r)} \tag{2.9}$$

Where R_L is loss resistance which corresponds to the antenna loss which should be minimized, and R_r is the radiation resistance which should be maximized. In practice, this value ranges between $50\% - 65\%$ and directly dependent on the matching of the antenna to the feeding network. Some of the energy is dissipated as heat inside the antenna, therefore the efficiency is degraded.

2.3.3 Radiation Pattern

The radiation pattern of an antenna is a plot of the far-field radiation as a function of the spatial co-ordinates which are specified by the elevation angle θ and the azimuth angle ϕ. More specifically it is a plot of the power radiated from an antenna per unit solid angle which is nothing but the radiation intensity[3]. Let us consider the case of an isotropic antenna. An isotropic antenna is one which radiates equally in all directions. If the total power radiated by the isotropic

antenna is P, then the power is spread over a sphere of radius r, so that the power density S at this distance in any direction is given as [11]

$$S = \frac{P_r}{area} = \frac{P_r}{4\pi r^2} \tag{2.10}$$

where P_r is the power radiated by the antenna, and r^2 is the spherical radial distance. Accordingly; the radiation intensity for the isotropic antenna, which is nothing but the power radiated per unit solid angle(steredians), is the real part of power density, and can be written as:

$$U_i = Sr^2 = \frac{P_r}{4\pi} \tag{2.11}$$

An isotropic antenna is not possible to realize in practice and is useful only for comparison purposes. A more practical type is the directional antenna which radiates more power in some directions and less power in other directions. A special case of the directional antenna is the omni directional antenna whose radiation pattern may be constant in one plane (e.g.E-plane) and varies in an orthogonal plane (e.g. H-plane). The radiation pattern plot of a generic directional antenna is shown in Figure 2.5.

As the power density is dependent on the electric field strength; very often the E field is used to describe the antenna pattern and usually normalized to its max value.

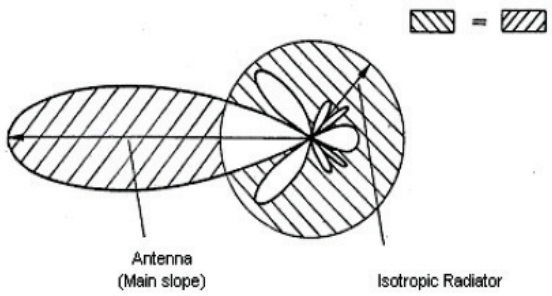

Figure 2.5: Radiation Pattern of a generic directional antenna

2.3.4 Directivity and Gain

The directivity of an antenna has been defined by [1] as the ratio of the radiation intensity in a given direction from the antenna to the radiation intensity averaged over all directions . In other words, the directivity of an isotropic source is equal to the ratio of its radiation intensity in a given direction, over radiation intensity of an isotropic source.

$$D_{max} = \frac{U_{max}}{U_i} = \frac{U(\theta, \phi)}{U_o} = \frac{4\pi U(\theta, \phi)}{P_r} \tag{2.12}$$

Where:

D_{max} is the maximum directivity

U_{max} is the maximum radiation intensity

U_i is the radiation intensity of an isotropic source

Directivity is a dimensionless quantity, since it is the ratio of two radiation intensities. Hence, it is generally expressed in dBi. The directivity of an antenna can be easily estimated from the radiation pattern of the antenna. An antenna that has a narrow main lobe would have better directivity than the one which

has a broad main lobe, hence it is more directive. The directivity of a $\lambda/2$ dipole antenna can be approximated by using the following empirical formula [11] at any elevation angle:

$$D = 1.64\ sin^3(\theta) \tag{2.13}$$

and at the max radiation plan $\theta = \pi/2$, the directivity reduces to $D = 1.64$, which is $2.23dB$.

To increase directivity one of the following methods can be used : Corner reflectors, reflector and multiple directors (Yagi Uda Like), and arrays.

The Gain and Directivity are two related characteristics of an antenna, they are equal for loss-less antenna($\eta = 1$). The Gain is expressed mathematically by :

$$Gain = \eta D \tag{2.14}$$

where η is the efficiency and its value between 0 and 1. The Gain G is less than the directivity due to the ohmic and other losses. G is expressed in decibels, which can be written as :

- dBi : relative to an isotropic antenna
- dBd: relative to half wave dipole antenna where 0dB is equal to 2.15dBi
- dBq : relative to a quarter wave whip antenna where 0dB is -0.85dBi

. and mathematically :

$$G_{[dBi]} = 2.15 + G_{[dBd]} \tag{2.15}$$

2.3.5 Voltage Standing Wave Ratio (VSWR) vs Return Loss (RL)

The efficiency of an antenna is a measure of the maximum transfer of power which take place between the transmitter and the antenna. Maximum power transfer can take place only when the impedance of the antenna Z_{in} is matched to that of the transmitter Z_S. If the condition for matching is not satisfied, then some of the power maybe reflected back and this leads to the creation of standing waves, which can be characterized by a parameter called the Voltage Standing Wave Ratio (VSWR). The VSWR is given by [9] as:

$$VSWR = \frac{1 + |\Gamma|}{1 - |\Gamma|} \tag{2.16}$$

where :

$$\Gamma = \frac{V_r}{V_i} = \frac{Z_{in} - Z_s}{Z_{in} + Z_s} \tag{2.17}$$

Where Γ is the reflection co efficient, Z_{in} is the antenna input impedance, and Z_s is the transmission line characteristics impedance.

The VSWR is basically a measure of the impedance mismatch between the transmission line characteristics reference impedance typically (50Ω) and the antenna impedance. The higher the VSWR, the greater is the mismatch. The minimum VSWR which corresponds to a perfect match is unity. A practical antenna design should have an input impedance of either 50Ω or 75Ω since most radio equipment is built for this impedance. The Return Loss (RL) is a parameter which indicates

the amount of power that is transferred to the load and does not return as a reflection. Hence the RL is a parameter similar to the VSWR that indicates how well the matching between the transmitter and antenna has taken place. The RL is given by [15] as:

$$RL = -20\log|\Gamma| \quad dB \tag{2.18}$$

For perfect matching between the transmitter and the antenna, $\Gamma = 0$ and $RL = \infty$ which means no power would be reflected back, whereas for $\Gamma = 1$ has RL= 0 dB, which implies that all incident power is reflected. For practical applications, a VSWR of 2 is acceptable, since this corresponds to a RL of -9.54 dB. In the simulation using HFSS we consider the S11 (scattering matrix parameter) equal to the RL as a measure for the antenna performance, and at the point of -9.54 dB(or -10dB) we measure the impedance bandwidth of the antenna.

2.3.6 Size, Weight, and Power (SWAP)

One extremely important aspect in antenna design is the SWAP, these parameters are investigated during the design of antenna and they are much dependent on the application and hence the requirements varies accordingly.

In Satellite communication for example, the SWAP of an antennas must be very small due to the space limitation in the space vehicle, which is designed to accommodate many component and the allowed space of antennas is limited. The power sources is also limited as well as the weight of the antenna, size and weight are directly translated to cost, thought it must be kept to minimum.

SWAP is also important when designing a mobile handset, the battery power is very limited and must be considered, in addition, the size and weight of the antenna are limited with in a space and shape such that they are hidden and integrated inside the casing.

On the other hand SWAP of antennas is of a secondary importance for applications in the fixed wireless base station. The AC power supply is available and the weight is not of a major concern, although the industry trend is going toward green BS designs where the power is a biggest concern.

2.4 Far Field Radiation of Wires and Dipoles

The analysis of wire or dipole antennas is a complex process, though it is suggested to consider small infinitesimal length of the antenna for analysis and finally add all the superposition to form the total antenna length. It is preferred to do this analysis using the spherical coordinate system as shown in Fig. 2.6, It is suggested

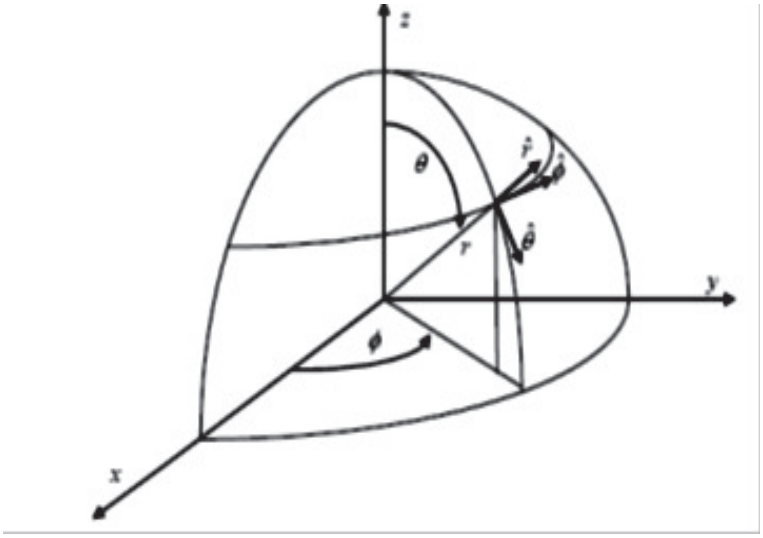

Figure 2.6: Spherical coordinate system used for analysis

by Balanis [13], that the z axis is taken to be the vertical direction and the xy plane is horizontal. The angle θ denotes the elevation angle and the angle ϕ denotes the azimuthal angle. The xz plane is the elevation plane $\phi = 0$ or the E-plane which is the plane containing the electric field vector and the direction of maximum radiation. The xy plane is the azimuthal plane $\theta = \pi/2$ or the H-plane which is the plane containing the magnetic field vector and the direction of maximum radiation, in our case $\phi = 0$ where ϕ is the angle between xz plane and the plane of max radiation. In this work we will use the same convention where the antenna will be placed parallel to z axis and the broadside radiation will be in x axis direction with max field is obtained at $\theta = \pi/2$.

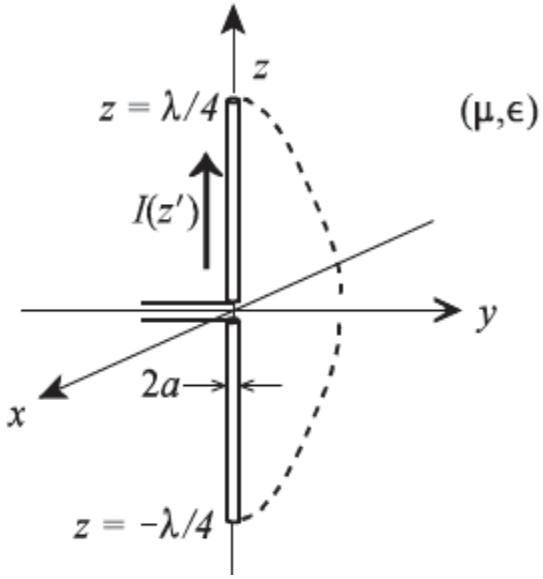

Figure 2.7: Dipole geometry

Using Fig.2.7, where a center fed dipole with radius a and length $l = \lambda/2$ and $kl = \frac{2\pi}{\lambda}\frac{\lambda}{2} = \pi$; placed along the z-axis, the following equations defines the electric and magnetic far fields when observation point is at distance r which is

much greater than the wavelength. At far field region, the waves will be a uniform plane wave and the center fed half wave dipole far fields can be given by:

$$E_\theta = j\eta \frac{e^{-jkr}}{2r\pi} I_o \frac{cos(\frac{\pi}{2} cos\theta)}{sin\theta} \tag{2.19}$$

$$H_\phi = j \frac{e^{-jkr}}{2r\pi} I_o \frac{cos(\frac{\pi}{2} cos\theta)}{sin\theta} \tag{2.20}$$

$$\eta = \frac{E_\theta}{H_\phi} \tag{2.21}$$

Where η is the free space impedance and equal to 120π or 377Ω. The radiation intensity function for the center fed dipole is also given by :

$$U(\theta, \phi) = \eta \frac{|I_o|^2}{8\pi^2} \frac{cos^2(\frac{\pi}{2} cos\theta)}{sin^2\theta} \tag{2.22}$$

And the directivity function is given by :

$$D(\theta, \phi) = 1.641 \frac{cos^2(\frac{\pi}{2} cos\theta)}{sin^2\theta} \tag{2.23}$$

At the plan of the max radiation ($\theta = \pi/2$) the directivity is 1.641 which is 2.15dB.

2.5 Theory of CR and CCR

The dipole antenna pattern is an omni-directional, with low gain, and narrow bandwidth. In order to increase such antenna gain, reflectors are used in many cases with different shapes and forms. A square 90^o corner reflector (SCR) is used

in this work to provide high gain and directive radiation, max gain is obtained when the vertex distance (s) defined between the location of the feed and the corner is $0.25\lambda and 0.7\lambda$.

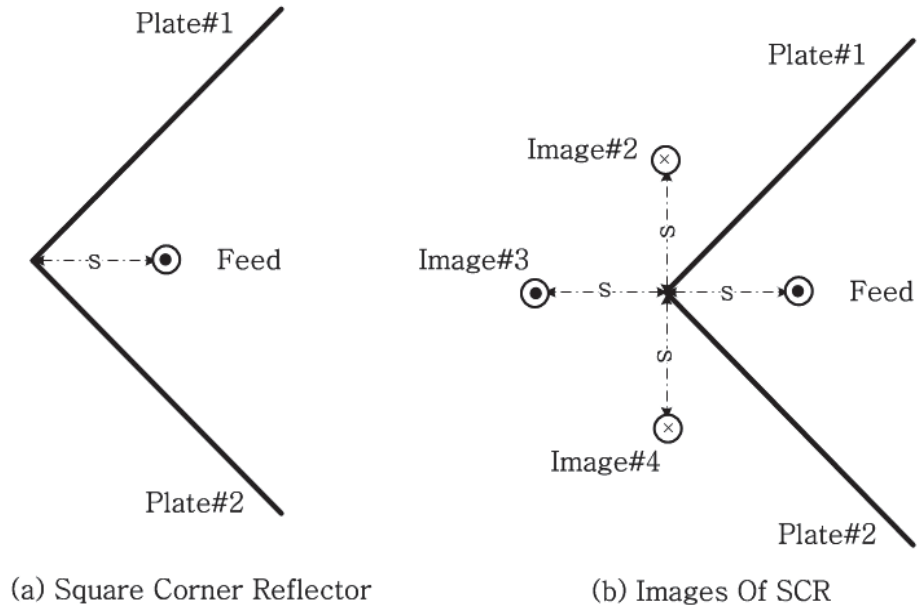

Figure 2.8: The square corner reflector and the feed images

In the analysis of the square corner reflector there are 3 images suggested by image theory [16]. From Fig.2.8, the feed will have an image (image 2) to satisfy the electric boundary conditions due to presence of the infinite plate 1, the same thing can be said for images 3 and 4. The driven antenna 1 and the 3 images have currents of equal amplitude. The phase of the currents in 1 and 3 is the same. The phase of the currents in 2 and 4 is the same but 180^o out of phase with respect to the currents in 1 and 3. The total field of the system can be derived by summing the contributions from the feed and its images [17]. To simplify the theory, the array factor is defined.

The main element and the images are divided two 2-elements linear arrays, and then add the contributions. The first linear array consists of elements 1 and 3 resulted in:

$$AF1 = 2cos(k * s * sin(\theta)cos(\phi)) \tag{2.24}$$

where $k = 2\pi/\lambda$ is the wave-number, and (s) is the vertex distance. The second linear array consists of elements 2 and 4 resulted in:

$$AF2 = -2cos(k * s * sin(\theta)sin(\phi)) \tag{2.25}$$

The negative sign indicates an out of phase currents in these elements. The addition of the two contributions gives the final array factor for the total array:

$$AF = 2cos(k * s * sin(\theta)cos(\phi)) - 2cos(k * s * sin(\theta)sin(\phi)) \tag{2.26}$$

Clearly, the array factor is highly dependent on the (s) value. Eq.2.26 is plotted using MATLAB and the (s) values was varied to study the effect on the H-plane radiation pattern characteristics when $\theta = \pi/2$. The results will be shown in Section 4.7.

For plane reflectors with 180^o the image theory depicts that the distance between the feed and the reflectors is the same as the distance between the image and the reflector. This will guarantee that the potential at any point on the reflector will be zero. For the case of cylindrical reflecting surface, the distance between the feed and the image is not symmetrical, the image is at a distance a^2/R from the

center of the cylinder. The antenna radiation pattern is a composite of the feed element radiated field and the array factor which spatially forms the radiation. Circular array formed by the images of the CR and CCR are investigated by Neff and Tillman[5], expressed the radiation pattern in forms of Bessel functions and cosine trigonometric identity which makes it possible to find the weighted coefficient for the currents of each element. The total CCR antenna radiated field is the antenna element radiation multiplied by the array factor, in the case of CCR the array factor is formed from two circular nested arrays as given by AlKamchouchi [1] and will be explained later in Sec 3.1.3.

2.6 Theory of Printed Antennas - Dipole Strip Antenna

2.6.1 Introduction

The Microstrip line is used for high frequency EM energy transmission since 1970's, its very suitable for transmission of EM energy for short distances within the electronic circuitry and between high frequency components. It is possible to be interfaced easily with MIC, on the same PCB. Microstrip lines are copper strips etched on top of a dielectric substrate.

It was noticed that the EM energy is confined under the copper strip line within the substrate, specially for high permitivity substrates. The EM energy tends to escape when the dielectric material refractive index ϵ_r changes, or at location of

bends in a form of unwanted radiation. For this reason low refractive index dielectric substrate are used as radiators in antennas, while the high refractive index substrate are used as transmission line in the MIC field. The Printed antennas in general and microstrip antenna in specific became very common in mobile communication as it became a very important part of mobile handsets and many other wireless application devices, due to their small size, easy fabrication, and conformable properties.

The first microstrip antenna was proposed by Deschamps in 1953. After development of printed board technologies. In 1970, Munson and Howell has developed the first practical antenna using the microstrip line. There are many layouts [13] found for the microstrip lines used as antennas, the most popular is the rectangular, dipole and circular. The layout is decided by the application and the targeted design, where dimensions are the most important.

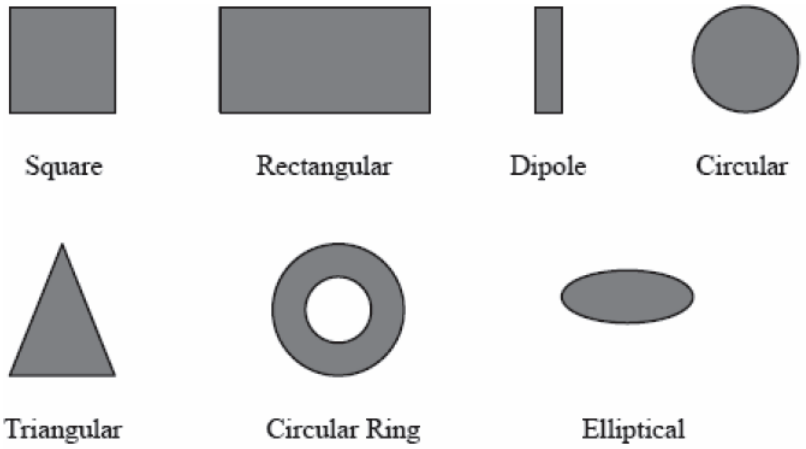

Figure 2.9: Printed Antenna different layouts.

Fig.2.9 shows layout of different patches used in micro-strip antenna[13]. The Rectangular patch is very well studied in literature, and some phenomena like

fringing is discussed, due to fringing effect the electrical length(Effective length L_{eff}) of the stripline is more than the physical length by a small value $\triangle L$. In addition the effective dielectric constant of the substrate is less than the dielectric constant ε_r due to the fringing effect, which is a result of presence of the field radiating in the substrate and air, as a result of the field not confined between the ground plane and the strip line. Fig.2.10 shows the fringing effect which causes the radiation. To enhance the fringing fields from the MSA which basically ac-

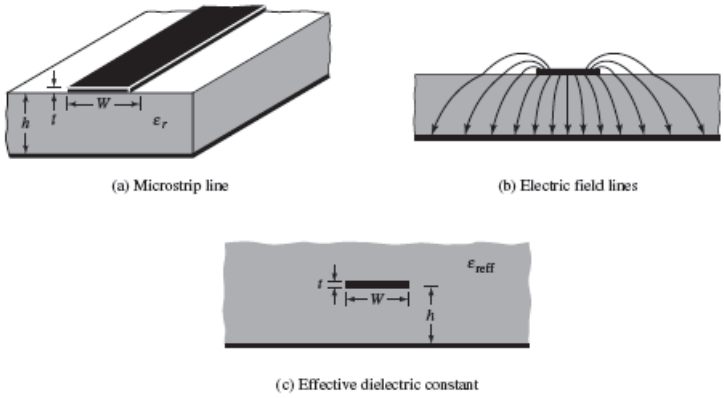

Figure 2.10: Microstrip line side view with fringing fields.

count for the radiation, the width of the patch W or the thickness of the substrate h can be increased, or dielectric constant ε_r can be decreased[13]. Increasing h also can enhance the impedance bandwidth, however it has a drawback as well. Surface wave will be excited at high thickness substrates, and will degrade the radiation efficiency. Rectangular patch analysis is very similar to the strip line printed antenna proposed in this thesis, and the strip line theory will also be introduced. The dielectric constant ϵ_r plays a major role in the overall performance of a printed antenna. It affects both the strip line width, in terms of the charac-

teristic impedance and the length resulting in an altered resonant frequency. We have used a semi rigid Duroid substrate in our case. In addition Duroid has a high loss tangent and is highly frequency dependent.

The bandwidth of the patch antenna depends largely on the permittivity (ε)and thickness of the dielectric substrate. Ideally a thick dielectric lower permittivity (ε) low insertion loss is preferred for broad band purpose.

Strip dipole antenna also uses the concept of strip lines for omni directional radiation. Its basically made of two strip lines etched on top of the substrate and fed directly from the gap. The length and width of the strip line determines the input impedance at the gap and it therefor determines the resonance frequency of the dipole. The use of strip lines requires having a ground plane at the bottom of the substrate, however this can be removed to obtain an omni directional radiation pattern. In our proposed design the ground plane is removed and replaced by a cylindrical reflecting surface at distance 0.25λ from the substrate. The printed strips of the dipole can also be placed opposite sides of the substrate at the top and the bottom, and fed by parallel transmission line, like the work done [18].

2.6.2 Printed Antenna - Pros and Cons

There many attributes that have made the printed antenna in general and dipoles in particular, a popular radiator used in many applications, although it also have some constraints.

1. PA are light weight, small volume and low profile planar configuration.

2. The PA can be conformed to non-planar surfaces as well.

3. Low fabrication cost due to use of PCB and mass production.

4. Supports linear and circular polarization

5. They can be integrated with MIC on the same PCB boards and they can be compact for use in mobile communication and handsets.

6. They support broad band with dual and triple frequency bands.

Despite the advantaged of printed antenna which made it preferred feed system for many application, there are few drawbacks associated with using it in some other applications, these drawbacks were discussed in many contexts and compared to conventional. Huge amount of research found in literature that address these limitations and propose designs that compensates for the low performance, below are the main disadvantages experienced when using printed antenna :

1. Narrow bandwidth; typically 1% to 5% which limits its use for widespread applications.

2. Low gain

3. Low power handling capability

Many techniques were found in literature that increases the bandwidth of the printed antenna, among them increasing the thickness of the substrate, without introducing surface waves. This technique increases the surface waves which affects the power efficiency and results in a negative effect on radiation pattern and

polarization purity. Surface waves can be eliminated by using cavities. Arrays are also another way of increasing the PA bandwidth to some extent.

In high volume production of printed antenna, two techniques are used to produce printed antenna:

- Etching: which is a subtractive process that uses chemicals and can creates waste.
- Printing: which is and additive process and more economical, therefore reduce the copper material needed.

2.6.3 Applications of Printed Antenna

Despite the disadvantages of the PA, they were found very attractive in many applications, due to their attributes discussed earlier, PA were intensively used for missile for telemetry and control. Patch antennas used for ships and satellite communications links. PA is also used for pagers,RFID, GSM, GPS, biomedical and remote sensing applications.

2.6.4 PA Feeding Techniques

There are various types of feeding techniques for MSA that directly influence the input impedance and the antenna characteristics. Due to its importance, these techniques are well studied in literature, some of these techniques are :

1. Co axial probe

2. Microstrip line

3. Electromagnetic or aperture coupling

4. Co planar wave guide feed where no direct contact between the patch and the feed line.

The first excitation technique will be used in this research for the printed dipole antenna feeding system. The other indirect feeding techniques are mainly suitable when thick substrate is used to gain more BW.

2.7 Broadband Antenna

In today's modern communication systems every applications is standardized to use a range of frequency spectrum, and it became very common to have these systems co exists in the same physical location or user device. It is a necessity that the same communication systems cover different frequency bands, similar to the case in personal wireless communication systems. 2G/3G/4G are currently built on the same physical structures and mean to cover the same zone. Due to that it became very crucial that the antenna system covers a wide range of frequency so that it supports these frequency band, hence rise the necessity for broadband antenna.

Defined by Sutuzman and Thiele [12], the antenna is broadband if the impedance and the pattern don't change over an octave($f_U/f_L = 2$) or more. Such antennas require that the structure dose not emphasis abrupt changes in the physical

dimensions involved , but uses smooth boundaries. Normally smooth physical structures produce patterns and impedance that also change smoothly with frequency.

Often, the bandwidth of narrow band antenna is expressed as percentage as below [12] :

$$BW = \frac{f_U - f_L}{f_c} * 100 \tag{2.27}$$

A half wave dipole has a BW typically between 8% to 16%, determined from the curve of scattering parameter S11 at $VSWR < 2$ using the points f_U and f_L.

The antennas that have traveling wave on them rather than standing wave, operates at wider range of frequencies, one type of such antenna is the resonant antenna. Antenna performance study involves extending the narrow band antenna to operate as wide band. In this work the printed dipole which is a narrow band width is optimized and modified to provide a wider range of frequency close to 1.3GHz. In addition, the radiation pattern is not changing over the bandwidth. Many 3GPP frequency bands used in today's Mobile communication systems are covered in that range of frequencies.

2.8 WiFi and 3GPP standards

Wi-Fi is aimed at use within unlicensed spectrum. There are a number of unlicensed spectrum bands in a variety of areas of the radio spectrum. Often these are referred to as ISM bands - Industrial, Scientific and Medical, and they are used in many applications: from microwave ovens to radio communications[19].

The WiFi radio enables users to access the radio spectrum without the need for the regulations and restrictions that might be applicable on some other parts of the spectrum. The drawback is that this spectrum is also shared by many other users and as a result the system has to be resilient to interference.

There are two main bands. The first is often referred to as the 2.4 GHz band, this spectrum is the most widely used of the bands available for Wi-Fi. Used by 802.11b, g, n. It can carry a maximum of three non-overlapping channels. The second is 5 GHz band or 5.8 GHz band provides additional bandwidth, and being at a higher frequency, equipment costs are slightly higher, although usage, and hence interference is less. It can be used by 802.11a,n. It can carry up to 23 non-overlapping channels, but gives a shorter range than 2.4 GHz.Fig 2.11 shows the frequency spectrum and channels allocated by standard[19]. Due to the limited availability of channels and the huge deployments of WiFi transceivers, the WiFi spectrum must be reused such that a high level of interference is expected. For that directional antennas are needed to limit the radiation of energy in directions only needed and prevent interference in all direction for other users [19].

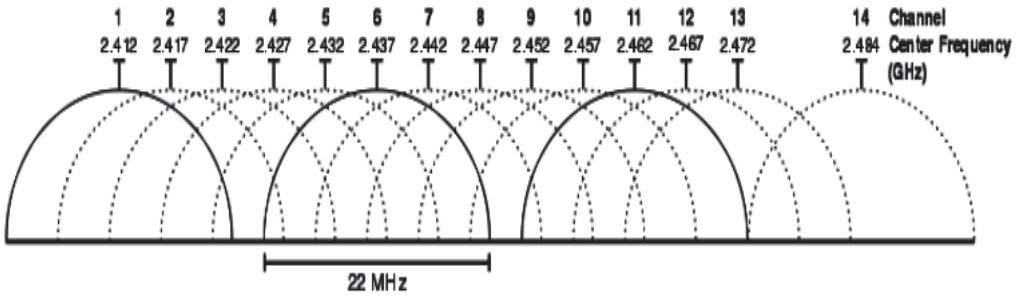

Figure 2.11: 2.4G Channel allocation for WiFi

In addition to the 802.11 standards being used for temporary connections, and for temporary Wireless Local Area Network, WLAN applications, they may also be used for more permanent installations. In offices WLAN equipment may be used to provide semi-permanent WLAN solutions. Here the use of WLAN equipment enables offices to be set up without the need for permanent wiring, and this can provide a considerable cost saving. The use of WLAN equipment allows changes to be made around the office without the need to re-wiring [19].

In this thesis the proposed antenna will be used as a directional antenna for WiFi IEEE802.11b,g,n. Historically; the WiFi hot-spot uses an omni directional antenna, that was possible due to low penetration of usage of WiFi applications. Currently, most of the portable devices consists of WiFi radio receiver and an omni antenna, that create a level of interference between users and depicts that we should use directional antenna to provide immunity against interference due limited number of channels available for users and large number of users that coexists in one place. Available current directional antenna are mainly panel antenna which is an array of rectangular patch.

The 3GPP(Third Generation Project Partnership) is a standard organization that aims to regulate the operation and development of wireless broadband communications. As seen in Fig.2.12, the 3GPP puts standard and regulations that controls the wireless communication industry. The system suppliers are forced to follow certain standard across the global space. 2G, 3G, LTE road map for

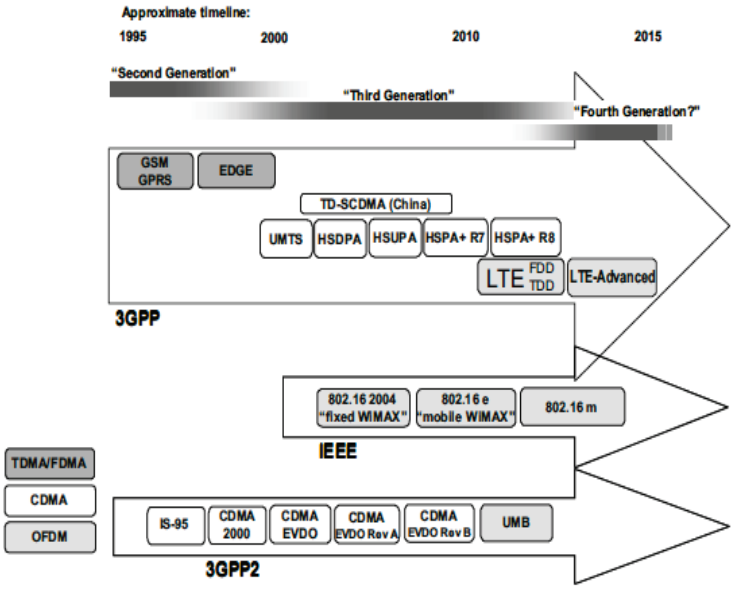

Figure 2.12: Development of 3GPP standard over years

capacity, frequency bands, and network architecture are well defined by standard and hence unified protocols is used for different continents [20].

There are three main directions in the standard field: 3GPP regulating the Europe and Middle east and North Africa, the second group is working's on North and south America which is the 3GPP2 group, and the historically known IEEE which is working's the WiFi and WiMax standards. The standards bodies are 2-3 years ahead of any development in wireless communication aspects[20].

The proposed antenna is going to be wide band and covering the range of frequencies that supports applications of both IEEE WiFi 802.11x, and the 3GPP applications like 3G/4G different bands.

CHAPTER 3

LITERATURE REVIEW

Antennas and their properties have became a wide area of research since a very long time. Some research and publications deals with the design of new antenna structures and shapes for new applications. Others are addressing a specific detail or an improvements introduced in the performance characteristics of the antenna like gain, radiation pattern and input impedance. In this chapter, we will summarize the research publications found in literature concerning our work which are divided in two categories. The first is related to corner reflector while the second is concerning the printed dipole. Further; a survey was done to collect some information about the available directional antenna found in market provided for the WiFi network applications.

3.1 CR and CCR related work

To obtain the fields along the axis of the CR, two approaches found in literature, and discussed by Shell in his report:

- Physical optics approach
- Method of images

The second was originally used by Niff and Tillman [5] in an attempt to reduce the complexity of the formulation analyzed and produced by Kraus[16].

3.1.1 V-shaped CR

Kraus [16] has suggested that a V shaped corner reflectors is essentially made of two conducting infinite planes joint at the corner with an angle α which is any sub multiple of π. The structure shown in Fig. 3.1 was analyzed and tested, found to provide higher gain at the intended direction of 2dBi compared to plane sheet. The driven element which is typically a dipole is mounted in the plane bisecting the corner at vertix distance S. The case when $\alpha = 180$ is the plane sheet and is considered a limiting case for corner reflector. It was shown by Brown that the gain is 7dB compared to free space dipole.

The CR is investigated using image theory, the reflecting planes are assumed to be infinite in length and perfectly conductive. In addition, array theory is used to analyze the field patterns resulting from the images. For a square CR with $\alpha = \pi/2$, we will have one radiating element and three images as shown Fig.3.2. Kraus has laid down the fundamentals and theory of CR, and gave few recommendations in the design of corner reflector. S which is the distance from the feed to vertex, has a limiting value after which the CR will generate multiple lobes. For 90^o CR this value is in the range of $0.25\lambda - 0.7\lambda$. The power gain or

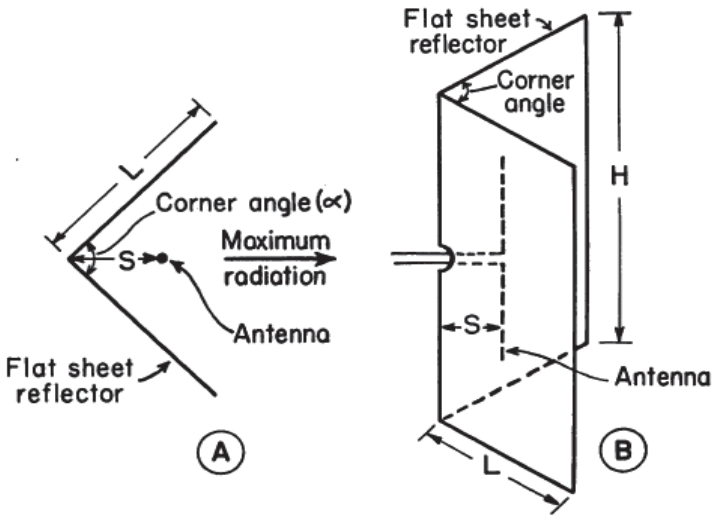

Figure 3.1: V Shape CR: 2D and 3D view with Images

gain for CR can be mathematically given by [16] :

$$PowerGain = 4\{\frac{300^o}{\alpha}\} \tag{3.1}$$

where α can be a sub-multiple of π. For 90^o CR, the theoritical power gain from Eq.3.1 is equal to 13.3dB.

3.1.2 The Design of CR

Niff and Tillman [5] re optimized the formulation of CR done by Kraus [16] which were found cumbersome and difficult to design an antenna accurately. As highlighted by Kraus and others[1][21] [6] , the CR angel $\alpha = \pi/n$ where n is any integer but not zero, the theory of images will be used to find the field along the CR axis as a result of the reflecting planes. The images form a virtual circular array of 2n equidistant elements and π radians of current phase shift between

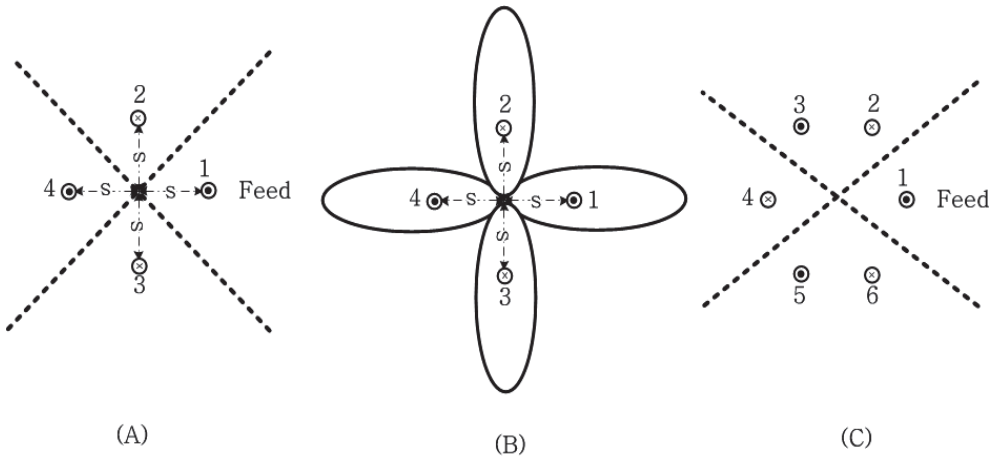

Figure 3.2: (A)Driven dipole with 3 image elements of SCR. (B) with 4-lobed pattern of this configuration. (C) Arrangement of images for 60-degree corner reflector.

adjacent circular array elements. The objective is to simplify the mathematical expressions of the array factor of the circular array.

Fig.3.3 shows a circular array of images produced by a CR with $\alpha = 60^o$, n=3. If the array contains number of elements m (m=2n), the current in each element is given by :

$$I_i = \frac{I_o}{m} exp(j[\omega t + (\frac{2\pi}{m})ni]) \tag{3.2}$$

and the field from each element is :

$$E_i = \frac{I_o}{m} exp(j[\omega t + (\frac{2\pi n}{m})i + \frac{2\pi}{\rho} sin(\theta) cos(\phi - \frac{2\pi}{m} i)]) \tag{3.3}$$

The above equation can be expressed in terms of Bessel(of first kind)and trigonometric functions, which can be simplified as :

$$E = 2I_o e^{j\omega t}[j^n J_n(z) cos(n\phi) + \sum_{k=1}^{\infty} j^{n(2k+1)} J_{n(2k+1)}(z) cos(2k+1)n\phi] \tag{3.4}$$

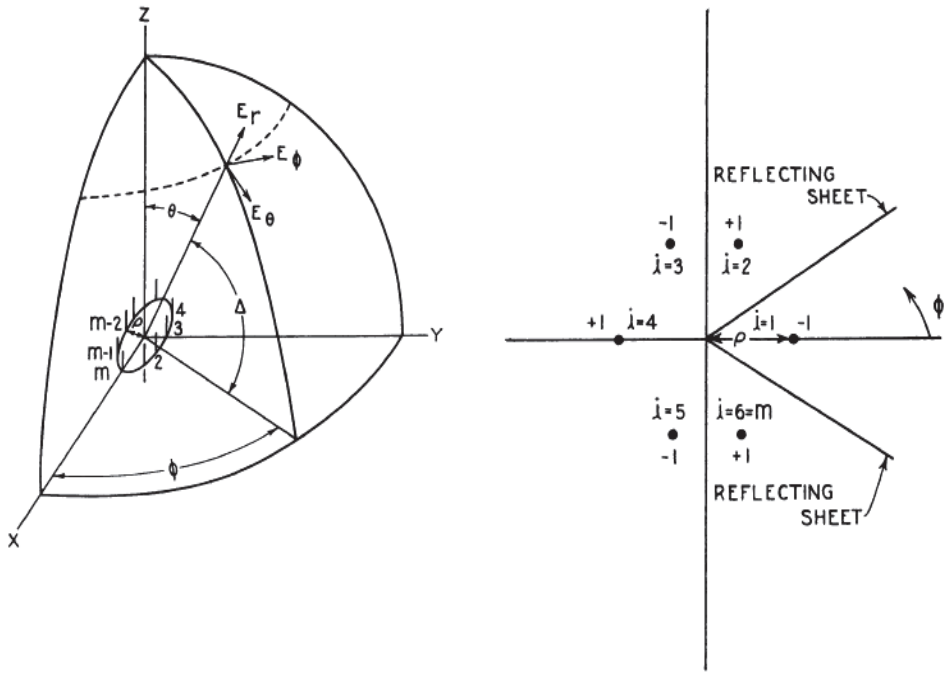

Figure 3.3: 3D and 2D views of Circular array

This is a simplified expression for the array factor in the plane of the array at max radiation($\theta = \pi/2$), where $z = 2\pi\rho/\lambda$. The same design process will be used later to design the CCR. If we are designing a CR with $\alpha = 60^o$, then n=3, and Eq.3.4 will be reduced to :

$$E = 2I_o e^{j\omega t}[j^3 J_3(z)cos(3\phi) + j^9 J_9(z)cos(9\phi) + j^{15} J_{15}(z)cos(15\phi) + ...] \quad (3.5)$$

And for our case of SCR; $\alpha = 90^o$, n=2 and Eq.3.4 is reduce to :

$$E = 2I_o e^{j\omega t}[j^2 J_2(z)cos(2\phi) + j^3 J_3(z)cos(3\phi) + j^5 J_5(z)cos(5\phi) + ...] \quad (3.6)$$

We have considered the first three terms of the series, but for more accuracy we can include more terms, although they will not be of much significant. We can conclude that the authors have provided an easy design method for CR with any

corner angle. The array factor for any CR antenna can be finally given by a simple mathematical expression:

$$E = KJ_n[\frac{2\pi\rho}{\lambda}sin(\theta)]cos(n\phi) + residual\ terms \tag{3.7}$$

3.1.3 Cylindrical Corner Reflector

Al Kamchouchi[1] suggested a modification on previous models of CR investigated by [16][5] . Adding a cylindrical reflecting surface to the V shaped CR, created a new group of images which forms a new circular array.

Modification on V-Shape CR

The ordinary CR suggested by Kraus [16] is modified by adding a new cylindrical reflecting surface with radius (a), as shown in Fig.3.4. The addition of this reflecting surface resulted in formation of new circular array of images with radius a^2/R. The distance between the feed and the apex is specified by R.

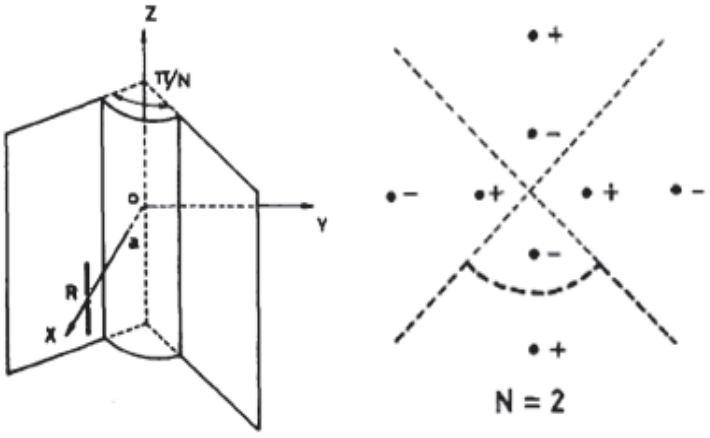

Figure 3.4: 90^o CCR: 3D and 2D view with Images

The structure is analyzed and tested, found to provide 2dB enhancement on the ordinary CR. The array factor at the plane of max radiation $\theta = \pi/2$, consists of 2 groups of circular array with 4 elements each, and the array factor is given by :

$$E(\pi/2, \phi) = 4sin(\alpha cos(\phi))sin(\gamma cos(\phi)) - 4sin(\alpha sin(\phi))sin(\gamma sin(\phi)) \quad (3.8)$$

where :

$$\alpha = \frac{2\pi}{\lambda}\frac{R^2 + a^2}{2R} \quad (3.9)$$

and:

$$\gamma = \frac{2\pi}{\lambda}\frac{R^2 - a^2}{2R} \quad (3.10)$$

The result is showing a clear dependence on the radius of the newly added cylindrical surface and the distance from the corner to the radiating element.The radiation beam is shaped accordingly and the impedance is controlled by varying both parameters.

Recently, the modified CR is also restudied by[22], where additional cylindrical reflectors are added, 3 or more reflecting surfaces can be sued to increase the images and though increase the antenna gain. A 60^o CCR with 3 cylindrical surfaces has shown an improvement of 5dB over the CCR suggested by Al Kamchouchi.

Modification on 3D CR

The second modification suggested by Al Kamchouchi is adding a cylindrical surface as an extension to the 3D CR investigated by Ingaki [21]; the result is adding

a 6.5dB gain over ordinary V -shape SCR.

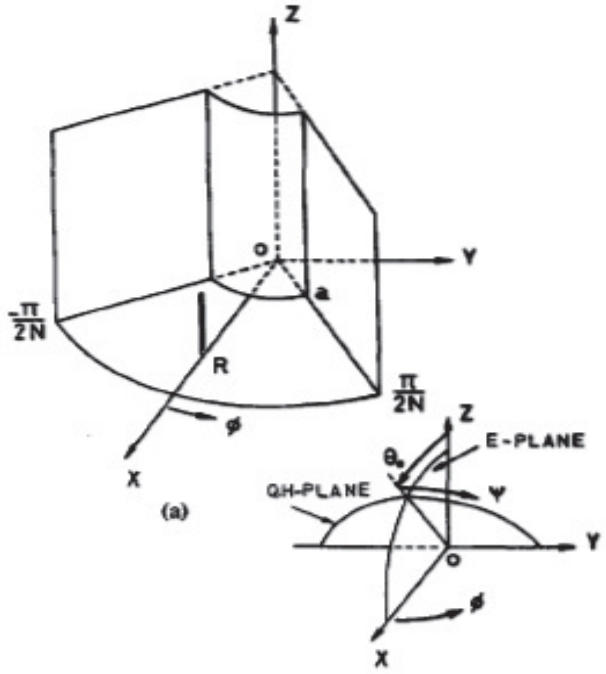

Figure 3.5: 3D CR modified to 3D CCR

The structure consists of a forth reflecting surface with a $3\lambda/4$ mono pole feed element. The array factor of the two E and quasi-H planes are having the following terms, for E plane:

$$E_2(\theta, 0) = 4sin(\alpha sin(\theta)).sin(\gamma sin(\theta)) \tag{3.11}$$

and for quasi H plane:

$$E_2(\psi) = 4sin[\alpha sin(\theta_o)cos(\psi)]sin(\gamma sin(\theta_o)cos(\psi))) - 4sin[\alpha sin(\psi))sin(\gamma sin(\psi)] \tag{3.12}$$

The reason for the name of H plane as quasi is that this type of antenna doesn't give a broadside radiation in the $\theta = \pi/2$ plane, but it is in the range of 30^o to 50^o.

3.1.4 Rad. Characteristics of Corner Array

Ragheb et. al [23] presented an optimization on the design investigated by Shell 1959, which is a corner reflector fed by array of dipoles placed on the axis of the CR, or at any position off axis at angle α_m from the axis as illustrated in Fig.3.6. This provides higher directivity based on array of dipoles. The work addresses the mutual coupling, the arbitrary angle for CR, and the off axis positioning of the dipoles to complete the investigation done by Shell in his report. The corner angle ψ is also left arbitrary, and at any point in space $P(r, \theta, \phi)$, the field is give by Eq.3.13, The total array radiation pattern is given by a set of mathematical

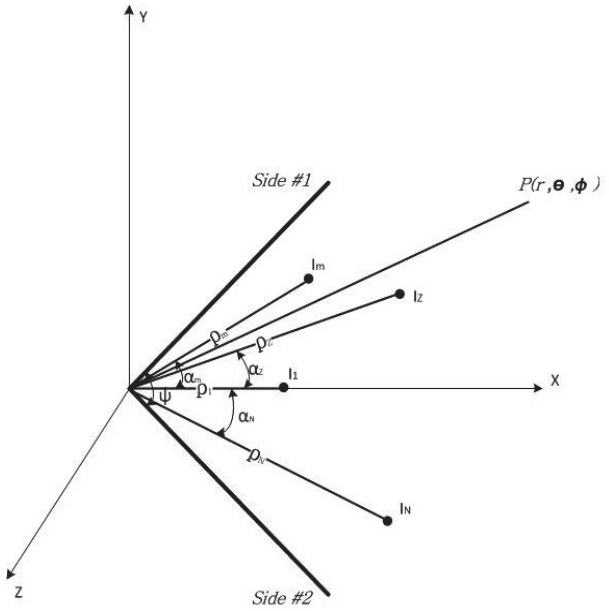

Figure 3.6: CR with array of half wave dipoles on/off axis

equations:

$$E_\theta = \frac{2j\omega\mu H}{4\pi}\frac{e^{-j\beta r}}{r} sin(\theta) S(\theta,\phi) \tag{3.13}$$

where :

$$S(\theta,\phi) = \frac{8\pi}{\psi}\sum_{m=1}^{\infty}(-1)^{n\pi/2\psi} I_m sin(n\pi(\frac{\phi}{\psi}+\frac{1}{2})) \tag{3.14}$$

and:

$$I_m = \sum_{n=1}^{\infty} J_{n\pi/2\psi}(\beta\rho_m sin(\theta) sin(n\pi(\frac{\phi}{\psi}+\frac{1}{2})) \tag{3.15}$$

The main parameters of the design are : corner angle ψ , distance from the dipole to the corner ρ_m , the excitation current I_m , and the dipole radial angle α_m. The above equations are simplified assuming that the array of dipoles are placed on the axis of the CR, where $\alpha_m = 0$. The excitation current is found using the array theory.

The same concept of dipoles array with CR is used recently by [24] to design novel antenna for application of portable WiFi BS antenna. This antenna increases the gain in azimuth plane(H-plane) and hence is also suitable for base station type application.

3.1.5 Design of CR Reactivily Controlled Ant.

Dimousios [24] suggested an electronically steerable beam scanning antenna operating on the 2.4GHz band. The proposed antenna uses the SCR with array of dipole as feed, same concept discussed and investigated by [23]. The antenna is essentially made of square CR, fed by an array of dipoles, in which one of them

is active and the other 6 are passive elements as shown Fig. 3.7. The passive elements are loaded with reactance that is electronically controlled by a separate circuitry to form a beam scanning mechanism by decreasing or increasing the electrical length of the dipoles. The EM coupling between the active center dipole and the other dipoles cause the gain to be increased in certain direction, and the CR will also reduces the side lobe level to the desired value.

This design is comparable to our proposed antenna. However its more complex, due to antenna size and dipole fixations. Also the external electronic circuits used to switch between the dipole reactance made the structure less favorable due to compactness, and less simplicity. The authors are using Genetic Algorithm to find

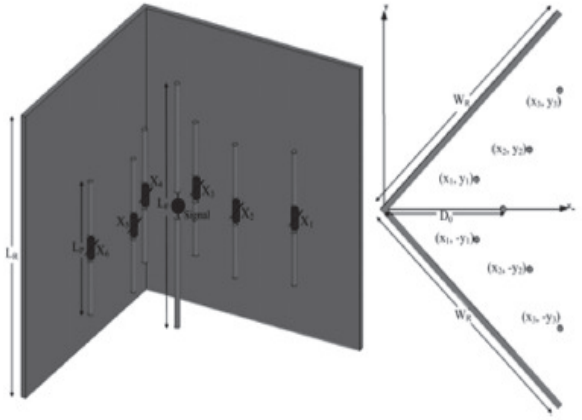

Figure 3.7: Reactively Controlled Array CR

the optimum location of the passive and active feed elements in addition to the value for the reactance, to provide scanning mechanism for the beam with max directivity. The same mathematical expressions discussed in [23] can also be used here, however others have used EM simulators to characterize the design due to their paramterization capability and computational speed in finding the optimal

performance.

3.1.6 A Novel Corner Reflector Antenna

Joseph and Mathew [8] have presented new type of corner reflector (CR) antenna with a rectangular dielectric feed. The proposed antenna provides a better performance with respect to radiation characteristics and impedance bandwidth compared to the standard corner reflector antenna with dipole feed when operates at X band range. A CR with corner angle α is fixed at the open end of a rectangular metallic wave guide Fig.3.8. A tapered rod rectangular dielectric feed is used, made of a low loss dielectric material(Polystyrene). The radiation characteristics

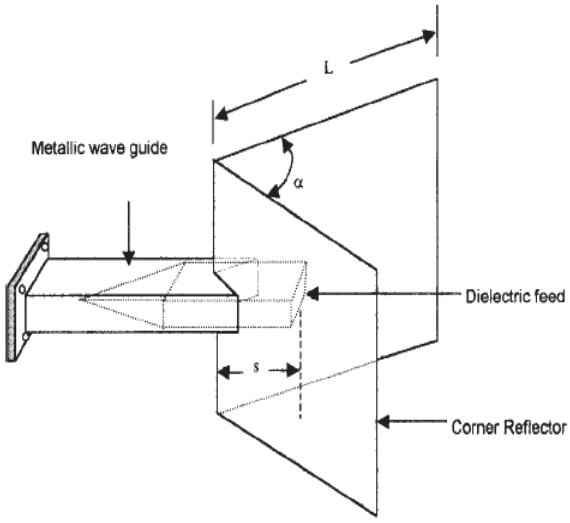

Figure 3.8: CR with tapered WG feed

and the bandwidth is studied after varying the corner angle, the operating frequency and the feed position. It was found that the H-plane radiation pattern is independent of the frequency and provided a low side lobe. These results are possible to obtain mathematically using a modified image theory, where the open

end of the WG feed is considered as a linearly polarized point source with field distribution equivalent to the aperture field of the dielectric wave guide.

One problem in this proposed antenna is that it works better at high frequency bands. At low frequency the WG size will be cumbersome, and difficult to attache to the CR plates.

3.1.7 CCR with Different feed

Abdulaziz [6] has replaced the commonly used feed for CCR by a vertical array of half wave dipoles. Fig3.9 shows the proposed antenna which is based on the CCR suggested by [1]. To enhance the radiation characteristics in the elevation plane(E-Plane), the conventional feed for CCR is replaced by a vertical array of half wave dipole placed longitudinally to the vertex plane. The mathematical analysis

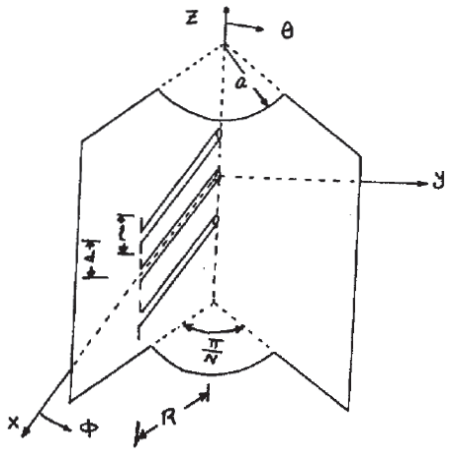

Figure 3.9: CCR with vertical array of half wave dipoles

used by [1] holds here. Image theory and array theory are used to provide a general form for the radiated electric field from this arrangement. It is essentially contributed from three components that are controlling the characteristics of the

radiation pattern and the input impedance of the antenna :

- Element Factor EF
- Array Factor ARF
- No. of driving elements NDF

The total radiated field based on the above components is given by:

$$E_\theta = K_1 * EF(\theta) * ARF(\theta, \phi) * NDF(\theta) \tag{3.16}$$

where :

$$K_1 = -(120\frac{I_o}{r})e^{-jkr} \tag{3.17}$$

$$EF(\theta) = \frac{cos(\frac{kl}{2}cos(\theta)) - cos(\frac{kl}{2})}{sin(\theta)} \tag{3.18}$$

$$ARF(\theta, \phi) = \sum_{n=1}^{N} sin(\beta cos(\phi_n - \phi)) * exp(j(\alpha cos(\phi_n - \phi) + n\pi)) \tag{3.19}$$

The feeding array can consist of either even or odd number of radiators, for odd number of feeding elements, =2p-1:

$$NDF(\theta) = \sum_{m=1}^{2p-1} a_m exp(-j\gamma(p - m)) \tag{3.20}$$

And for even number of radiating elements, M=2p:

$$NDF(\theta) = \sum_{m=1}^{2p} a_m exp(-j\gamma(p - m + 1/2)) \tag{3.21}$$

The constants α, β, and γ are directly dependent on the radius of the cylindrical surface and the distance between the feed and the corner. Later in chapter 5, the results of a Matlab code that simulates the radiation dependence on these two factors will be presented.

3.1.8 Optimized Design of CCR

Romo [25] presented an optimization to the CCR designed and investigated by [1] and[6]. The main aim of this work is to improve the performance of the CCR used for TV transmission. By using two new feeding systems: Yagi Uda antenna and another specially designed feed system. The design combines the CCR and the Yagi Uda to provide high directivity and high bandwidth antenna. The design

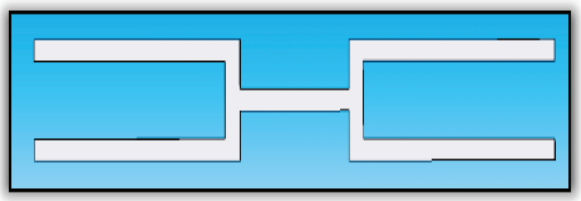

Figure 3.10: New Feed element suggested for CCR

consists of a new feed system other than the conventional wire dipole Fig3.10, which consists of planar sheets connected via a balun. The length of this balun varies between approximately 0.54λ at the lowest frequency and 0.99λ at the highest frequency of the bandwidth. Directivity gain is greater than 2dB compared to other dipole radiators.

The CCR with a 3 reflecting planes are made of grid wires to minimize the windload and increase the stability of the structure as shown in Fig.3.11b. The antenna

operates at the low frequency bands UHF/VHF and used for TV broadcasting.

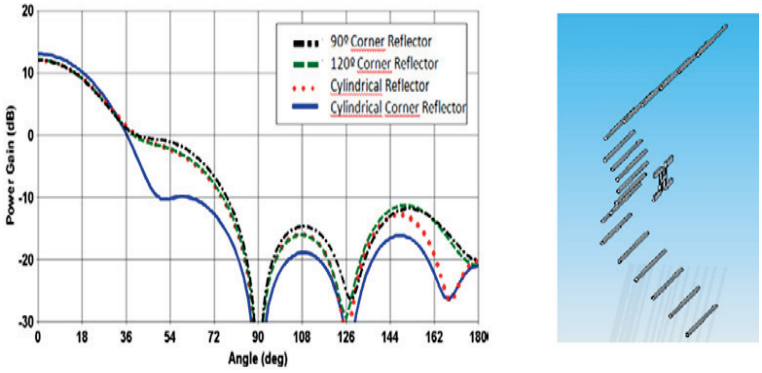

Figure 3.11: (a) 2D radiation pattern using different CR. (b) CCR using wire grid reflectors and different feed

The proposed antenna has shown an improved performance at the operating frequency. Higher gain and reduced side lobes level compared to conventional CR was obtained Fig.3.11a. Multiple configuration were tested covering different frequency bands and at different CCR dimensions. Among all different configurations of CR, the CCR was found to provide best performance with respect to power gain, directvity, HPBW, and impedance bandwidth.

3.2 Printed Antenna

3.2.1 Printed Dipole Antennas for WLAN Applications

Printed antenna is discussed in literature and used in many applications. Printed dipoles with omni directional radiation are uses extensively in almost all wireless communication devices, like mobile phones and laptops. There are many advantages for the printed antenna, although they have few drawbacks. The operating

bandwidth is usually low $1\% - 3\%$, further, they have low power handling capabilities. Due to that, it became a challenge for designers to mitigate this problem by using arrays. [2, 3]. The design of printed dipole antenna for higher operating bandwidth involves finding optimal strip width and length, substrate thickness, and proper dielectric constant. Usually low ϵ_r substrates are used to build antennas while high ϵ_r substrates are used for transmission via micro strip lines [15].

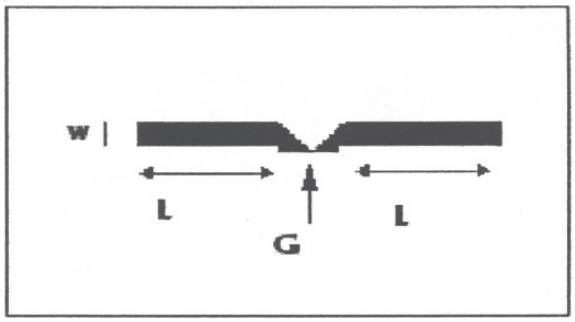

Figure 3.12: printed Strip Dipole

In [2, 3] the authors are designing a micro strip antenna that exhibits a high bandwidth and good E and H isolation in the broad side direction of radiation. Fig 3.12 shows the schematic of the dipole antenna. The variation of width and length of the dipole strip has a great influence on the resonance frequency and the input impedance. With optimal values for W=4mm and L=23mm, it was possible to achieve 13% bandwidth.

Printed dipoles are also used in base stations for wireless communications. This type of application requires the use of directional antenna. Dipoles in form of Yagi Uda array were designed and introduced by [26], one director and multiple reflectors are arranged to give an end-fire radiation pattern suitable for sector zone

applications.

3.2.2 Broadband sector Zone BS Antenna

In Tafiko [4] [27], a printed strip dipole on a thin dielectric substrate is designed and tested. The author presented a new antenna for wireless communication system base station and sector zone application. It is made of two series array strips fed by microstrip line, strips are printed on top and bottom sides of the substrate, as shown in figure 3.13. A flat or shaped reflector is placed under the array and used to increase the directvity of the antenna in the end-fire direction. The reflector dimensions has a big influence on the H-plane radiation pattern. The series

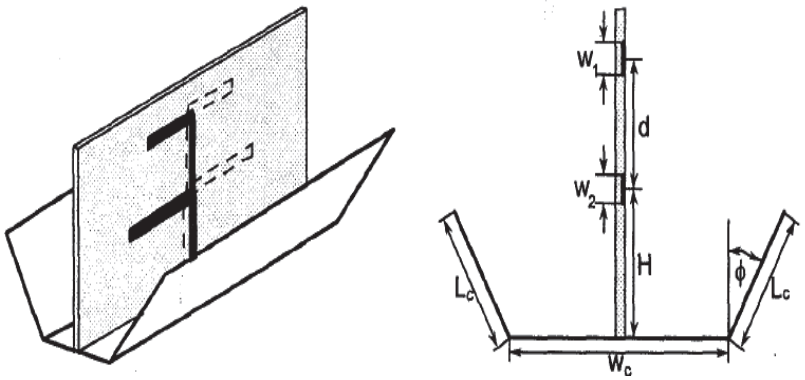

Figure 3.13: Printed Strip Dipole on top of a shaped reflector

fed, two printed strips placed on shaped reflector is designed and investigated. One challenge associated with this arrangement is the broad band impedance matching, it became very difficult process due to having the printed strips placed closed to the conducting reflector.

The radiation pattern is controlled by varying the L_c, W_c, ϕ , to provide the desired pattern shape in H plane, and a broad band impedance bandwidth with 30% at

$VSWR < 1.5$. Three different sectors angles in the H plane ($120^o, 90^o, 60^o$) were tried by changing the reflector parameters, and all have provided a satisfactory broadband 3dB bandwidth.

For arrangement shown if Fig.3.13, the radiating element consists of two strip dipoles of lengths L, with strip arms printed on both sides of a thin dielectric substrate. A distance d separates between the Strip dipoles and they are connected through parallel strip lines.

To analyze series-fed arrays of printed strip dipoles, the author has employed a modeling technique for the printed strips and the shaped reflector. An equivalent model based on the equivalent radius of cylindrical antennas is used, where the printed strip dipoles are transformed to circular wires with coaxial magnetic covers. This is conditional for narrow strips printed on an electrically thin dielectric substrate. Additionally; a wire-grid model representing the conducting reflector is used to analyze the antenna.

The shaped reflector afterword became very popular in the design of panel antenna for GSM base station, the author later on proposed a dual band broadband antenna after redesigning some parameters. Array of cross polarized dipoles are placed on the reflector, +45/-45 slanted dipoles are used to provide polarization diversity. A very similar idea is developed by Ericsson recently to provide an antenna for base station use[28]. The re modeling in this paper will be used to convert our proposed design to an easier case of CCR with wire feed for mathematical analysis of the radiation. This approach is simulated and found in match

with results of our proposed antenna.

3.2.3 Millimeter Wave Corner Reflector Antenna Array

In Nesic [18], the CR is used to further suppress the side lobe in the printed antenna array. A millimeter wave PA array is designed using pentagonal dipoles fed by symmetrical micro strip line. Eight pentagonal dipoles are printed on bottom and top of the substrate to give broadside radiation as shown in Fig.3.14. The array is designed to operate on 26GHz used for point to point or point to

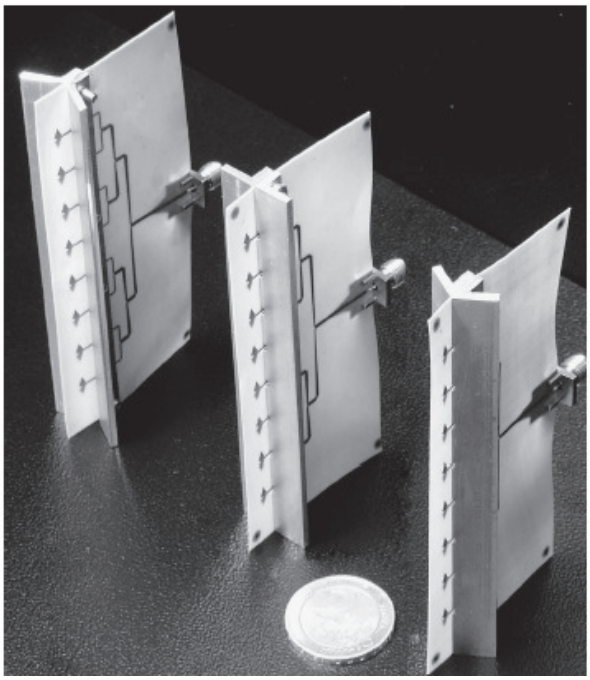

Figure 3.14: CR fed by axial array of Pentagonal printed dipoles

multi point microwave applications. The CR reflector provided a very narrow beam width (10^o) in the E plane. This design is very similar to the proposed design in [6], except that it uses different radiating elements from that used in conventional CR, in addition it supports higher frequencies in the millimeter range

with high side lobe suppression. In order to get the max array gain, the distance between dipoles is kept at 0.9λ to reduce the mutual coupling between adjacent antennas. The simulation of the antenna provides a very good performance. Table 3.1 below summarizes different performance parameters at different CR angles.

For the first time, this paper introduces a new concept for CR where the corner

Table 3.1: Simulated parameters at different CR Angle

CR α^o	Gain[dBi]	FSLA[dB]	F/B [dB]	$HPBW^E$	$HPBW^H$
127.5	19.4	13	33	6.9	54.6
180	16.6	13	31	6.9	109.5
255	14	12.9	22	6.9	182

angle ($\alpha > \pi$), the use of CR angle 255^o has a clear influence on the H-plane HPBW and increased it to around 180^o. This feature is important in some applications, while all other tried CR angles has achieved a very narrow HPBW in the E plane. The First Side Lobe Attenuation obtained is around 13dB for all CR angle cases with very good front to back ratio.

3.2.4 Conformal Mapping Technique

Conformal mapping technique have been investigated in [29][30]. A planar surface antenna or array can be mounted on a non planar surface like cylinder or cone similar to our proposal. Conformability of printed antenna on non planar surfaces became a very important merit that define the antenna characteristics. Most of real life surfaces are not planar and to mount a printed antenna on these surfaces became very challenging process.

The IEEE Standard Definition of Terms of Antennas defines the conformable an-

tenna as [14]: "Conformal antenna is defined as an antenna that conforms to a surface whose shape is determined by considerations other than electromagnetic; for example, aerodynamic or hydrodynamic". Usually, a conformal antenna is cylindrical, spherical, or some other shape, with the radiating elements mounted on or integrated into the smoothly curved surface.

Transformation of cylindrical surface to planar surface using conformable mapping technique is introduced. The authors have applied such techniques in studying a rectangular patch on cylindrical surface. The rectangular patch on a planar substrate is very well studied in literature and a closed form equations for the resonance frequency, input impedance and other antenna parameters are well developed. The main focus will be on the patch width, this parameter is the most affected by the cylindrical curvature. Fig3.15 shows the process.

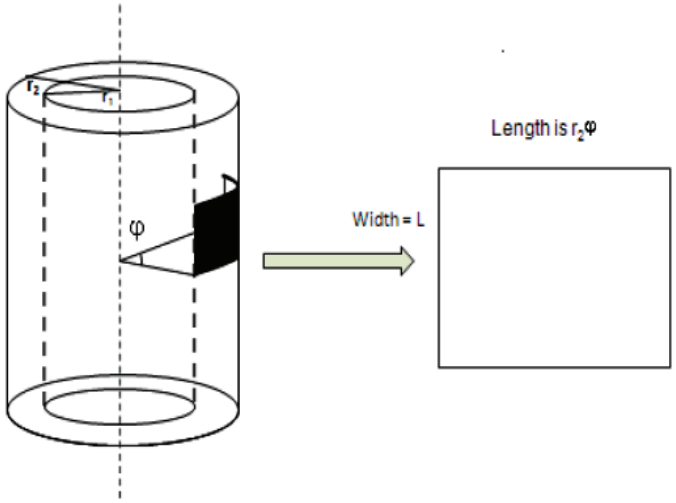

Figure 3.15: Equivalent patch width transformed

Transformation relation for the patch width W is developed as:

$$W^{'} = (r_1 + h) * \varphi \tag{3.22}$$

where r_1 is the radius of the cylinder , h is the cylindrical substrate thickness, and φ is the angle subtended by the patch along the central axis. Numerical examples were given and a simulation was done to prove the assumption that conformable mounted microscopic patch can be transferred as planar, and finally an empirical formula for the frequency ratio in case of planar and conformable antenna is given:

$$\frac{f_{conformal}}{f_{planar}} = 1.0856e^{-1.332(\frac{r_1}{L^{'}})} + e^{-3.527*10^{-6}(\frac{r_1}{L^{'}})} \tag{3.23}$$

where $L^{'}$ is the length of the transformed planar microstrip. The same above methodology can be applied in case of array. Therefore conformable arrays are possible to realize. This method can be applied in our proposed design, however the strip width suggested is narrow and has a small value compared to the circumference of the cylindrical structure. It is expected that the cylindrical curvature will have minimum impact on the frequency resonance and the matching of the printed strip dipoles. This will be proved by simulation and the results will be discussed.

3.3 WiFi Antenna Market Survey

Recently the WiFi standard as a short range communication started to gain more focus. WiFi transceivers are built almost in every personal communication device. Often, system is built using onmi directional antenna, only few special cases were built using directional antenna at the base station side. In this section we will investigate the available high gain antenna developed for WiFi. Many companies are specialized in WiFi products and the high gain antennas.

Figure 3.16: Different types of antennas found in the market

In the market, directional antennas are built based on batch antenna or wire dipole. Different antennas are studied in this work and compared so we assist the design of our proposed antenna. Fig3.16 shows some directional antennas found in the market provided by famous suppliers. They are differentiated by some characteristics parameters namely the radiation pattern, max gain, frequency band ,

Table 3.2: Directional Ant. Specs

no.	Name	Supplier	Freq. Range	Gain	Type
1	HAI15SC	Hawking Tech	2.4G	15dBi	Corner Ref.
2	Hawking	Hawking Tech	2.4G	14dBi	Microstrip Patch
3	ANT5195P-R	Cisco	5G	9.5dBi	Microstrip Patch
4	TEW-A014D	TrendNet	2.4G	14dBi	Microstrip Patch
5	Grid	Grid	2.4G	24dBi	Parabolic

and more importantly the size. The MIMO in many cases is needed and is a very important figure of merits. Table4.1 summarizes few antenna main specifications as a reference and for purpose of comparison.

Looking for simplicity, and low cost, the corner reflector is a very good choice, however the size makes all of the found models to be less attractive in deployments. In our proposal we have taken these issues in consideration such that we have matched the size, cost, simplicity, and high gain.

CHAPTER 4

ANTENNA DESIGN

A new design of CCR antenna is introduced here. The antenna consists of a 90^o corner reflector fed by a strip dipole printed on a quarter cylindrical substrate. Two parasitic elements has been added also in parallel with the dipole to broaden the bandwidth. The printed dipole is used to feed the structure and provide a wide range of design parameters that controls the radiation pattern, and bandwidth, at the same time keeps the structure simple and low cost. Design parameters of the printed strip dipole is based on transmission line model described in [13].

4.1 Printed Dipole Antenna Design

Many designs have been investigated and studied, while only few of them can be used as feed for our proposed antenna. Most of the dipoles investigated in literature used strip line feeding solution, while in the proposed design we use the probe feed at the center gab of the dipole strips. This is considered as challenge for the impedance matching and fabrication.

For the printed dipole to resonate at 2.4 GHz, and provides an omni directional radiation pattern since there is no ground plan involved. The design parameters are based on references [3][2][31]. First, substrate used is Duroid TM, with dielectric constant of 2.2, and thickness h= 1.6mm. The dipole strip width is w=4mm, and the quarter cylindrical radius is optimized to 0.6λ. The free space wavelength $\lambda = c/f$, where c is speed of light, and f is the resonance frequency of the antenna. The effective dielectric constant is calculated using the Eq.4.3. Eq.4.1gives L for the half wave Strip dipole based on [32][3][2][31]. Also, the formula for finding other calculated parameters can be found in [13]. Often, total dipole length is kept less than half wavelength to count for reactive fields in the near field region which are controlled by the length of the radiating element, and is approximately given by:

$$L = 0.47\frac{v}{f} \tag{4.1}$$

where ν is the actual propagation speed of wave in the dielectric which is given by:

$$v = \frac{c}{\sqrt{\epsilon_{eff}}} \tag{4.2}$$

and c is the free space light speed. Given the material dielectric ε_r , the substrate thickness h , and the resonance frequency f_r , the other antenna parameters can be found using the following steps:

- Calculate the effective dielectric constant ε_{eff} using the following equation

for $\frac{W}{h} > 1$ and selecting w=4mm, h=1.6mm :

$$\varepsilon_{eff} = \frac{\varepsilon_r + 1}{2} + \frac{\varepsilon_r - 1}{2}(1 + 12\frac{h}{W})^{-1/2} \tag{4.3}$$

- Calculate the effective propagating wavelength is :

$$\lambda_{eff} = \frac{\lambda_o}{\sqrt{\varepsilon_{eff}}} \tag{4.4}$$

- Calculate ΔL to count for Fringing effect:

$$\frac{\Delta L}{h} = 0.412\frac{(\varepsilon_{eff} + 0.3)}{(\varepsilon_{eff} - 0.258)}\frac{(W/h + 0.264)}{(W/h + 0.8)} \tag{4.5}$$

- Calculate the effective length:

$$L_{eff} = L + 2\Delta L \tag{4.6}$$

- Finally calculate the resonance frequency :

$$f_r = \frac{\nu_o}{2L_{eff}\sqrt{\varepsilon_{eff}}} \tag{4.7}$$

Where $\nu_o = 3x10^8 m/s$ is the speed of light in free space. Performing the numerical calculations, we found that: $\lambda_{eff} = 92mm$, and the strip dipole length is 45.5mm, the $\varepsilon_{eff} = 1.8491$, ΔL =0.745mm, and the resonance frequency is 2.42GHz. The width of the dipole strip radials is fixed to W=4mm.

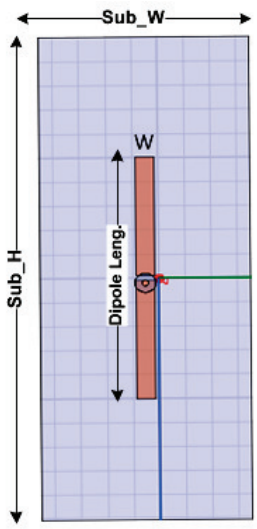

Figure 4.1: Printed dipole on a planar substrate model

We have chosen the dielectric semi rigid PCB for the substrate as Duroid(tm) with dielectric constant of 2.2 and thickness of 1.6mm. Dipole radials width can be found in [32][3][2] to be 4mm. The effective dielectric constant was found from the above equation as 1.8491. Dipole radial length is found based on the effective wavelength of the propagating wave ($\lambda_{eff} = 92mm$) at 2.4GHz equal 23 mm.

Table 4.1: Antenna Geometry

Designed Frequency	2.4 GHz
Dipole Radials Length	23 mm
Dipole Radials width	4 mm
Gap	1 mm
substrate height	1.6 mm
dielectric constant	2.2
Effective Wavelength	92 mm
Cylinder substrate Radius	0.687λ
Cylinder Reflector Radius	0.437λ
Cylinder Height	λ
Reflecting sheet HxL	$\lambda * \lambda$

Table 4.1 summarizes the different design parameters of the antenna based on

calculations, and will be used in the simulation and fabrication.

The design concept used for the cylindrical substrate , the thickness, strip dipole length and width, and the material remains unchanged. Cylindrical substrate radius is $R = 0.687\lambda$, and the substrate is placed at a distance of 0.25λ from the reflecting cylindrical surface. Printed dipole on a substrate provides a more rigid structure that the wire dipole type feeding system offers. The printed strips are fed from the gap between the two strips via a coaxial feed by using 50Ω industrial SMA connector.

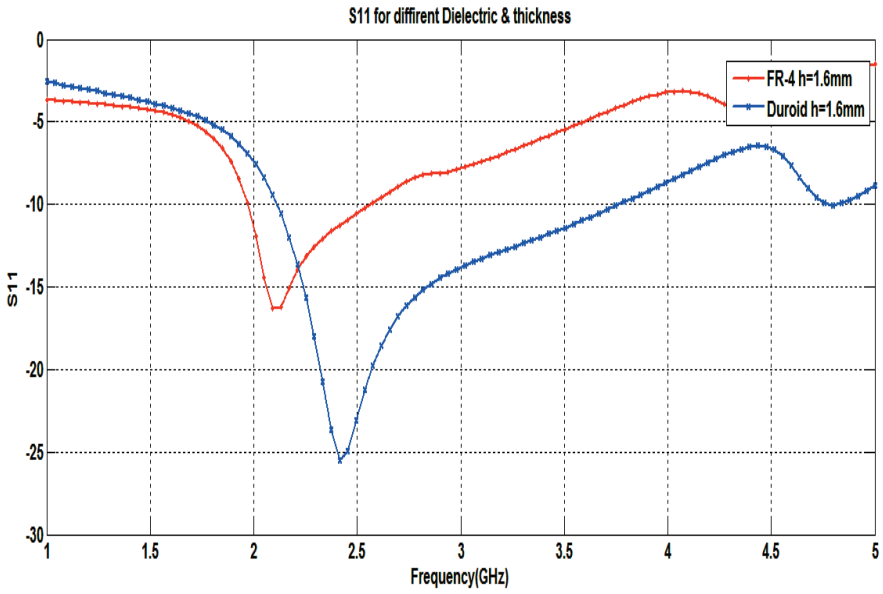

Figure 4.2: S11 for different substrate material: Duroid and FR-4

4.2 Effect of Substrate material and Thickness on design of PA

To study the effect of dielectric material on the resonance frequency and the input impedance, FR-4 epoxy substrate with relative permittivity of 4.4, relative permeability of 1, and dielectric loss tangent of 0.02 is used. The thickness and other parameters are kept unchanged. Fig.4.2 shows that the operational band is shifted towards the lower frequencies with increasing relative permittivity. Negative effect on the impedance matching of the antenna is also noticed since the antenna 3dB impedance bandwidth is reduced. The results we obtained are in agreement with the analysis done by [33], the effect of relative permittivity on the rectangular patch is similar.

To have an insight on the effect of substrate thickness on the PA performance, the thickness of the substrate is set to different values, and other parameters are kept unchanged. Fig.4.3 shows the effect of different thickness values on the operating frequency.

We can conclude that thickness of h=1.6mm or h=2mm using Duroid TM gives acceptable performance. However we will use semi rigid Duroid TM with h=1.6mm thickness in our future simulation and fabrication due to its availability in KFUPM laboratories.

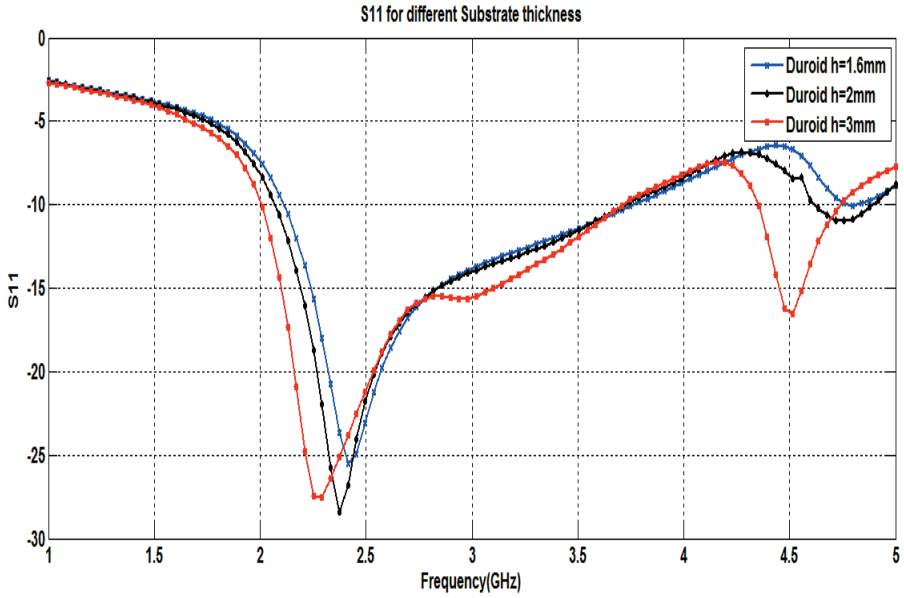

Figure 4.3: S11 for different substrate thickness

4.3 Effect of the Plates size

As per Kraus [16], the CR corner plates can marginally affect the radiation pattern in the E and H plane. Recommended values for plates length is $1 * \lambda$ to $2 * \lambda$. We have simulated both cases, the directivity is increased by small value. Fig.4.4 shows the radiation characteristics enhancement. Increase in Gain by 1dB is obtained, and a null of -35dB is introduce. In our fabrication later on we have used the smaller dimensions to keep the volume of the antenna small if possible. Of course we can always increase the plate size to obtain better radiation and directivity, but at expense of size.

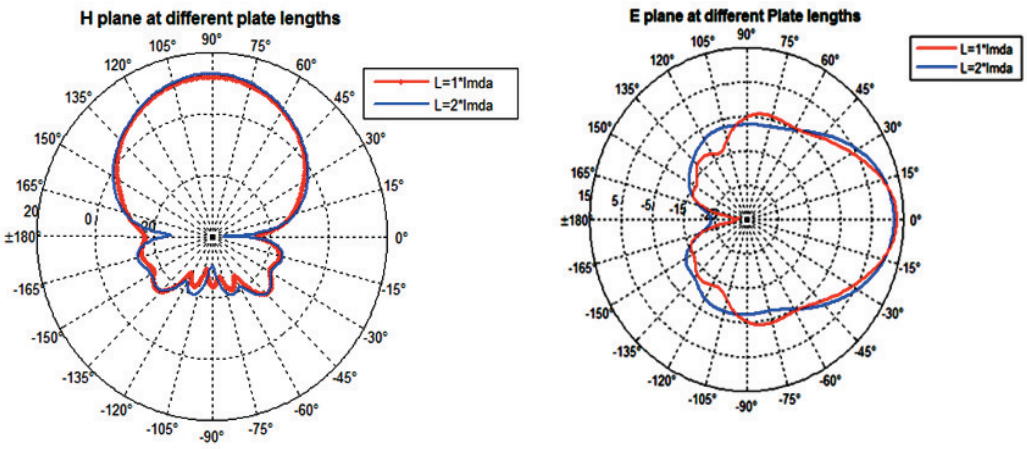

Figure 4.4: Gain for different CCR plate lengths

4.4 Broadband Antenna Design

In order to broaden the antenna bandwidth, two parasitic strips were printed in parallel to the strip dipole. The concept is inspired by the design in [34] in which a rectangular parasitic element is placed near the dipole arms. The electric field is coupled to the parasitic element, which becomes a radiator itself. This parasitic element is designed to have a length slightly different from the dipole arms to create extra resonance that increases the bandwidth of the antenna. Applying the same concept here, two thin lines (which act as parasitic elements) are added along the edges of the dipole arms. These lines and the dipole arms are placed on the same side of the substrate.

The design parameters of these parasitic elements were obtained using the simulation package HFSS. HFSS parametric function is used to search for optimal dimensions which produce the best broadband S11 graph. The parasitic elements insert a dip close to the 2.4G which allows the antenna to resonate at wide bandwidth [34].

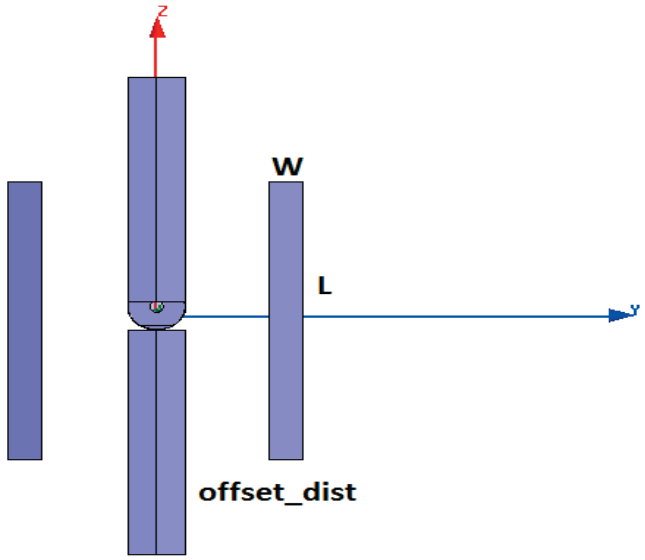

Figure 4.5: Optimal dimensions of the parasitic elements

Table 4.2 summarizes the dimensions of the parasitic elements, with optimal values.

Table 4.2: Parasitic Elements Geometry

Width of the parasitic strip	3 mm
Length of the parasitic strip	0.24λ (30 mm)
Offset from the radiator	(11.5 mm)

4.5 Conformable Printed Antenna

Printed antenna on a planar substrate (surface) can be considered to have reached its maturity, while the development of conformable antenna on a non planar surfaces lags behind. There is a critical need for numerical and analytically techniques to study the antenna performance when using more real world surfaces to build the antenna on, like cylinders, cones and spheres. The cylindrical shape can approximate most of the surfaces in real structures, in our work the printed

antenna strips are conformed on a quarter cylindrical outer surface, hence; we devote some of the discussion to this part. Theoretical work investigating the

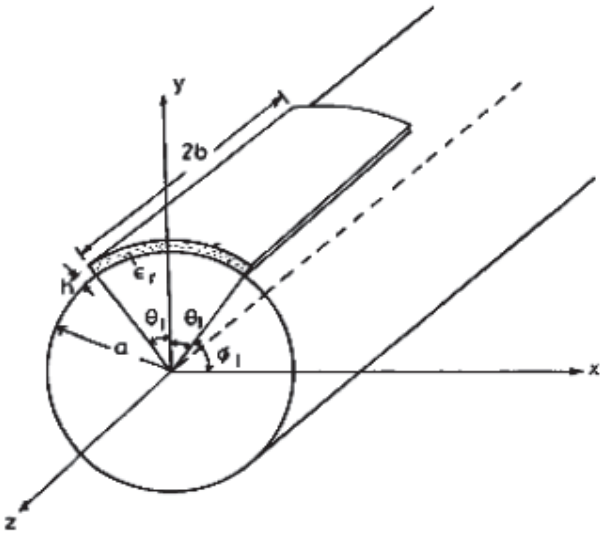

Figure 4.6: printed strip on a cylindrical substrate - conformable mapping

antenna performance parameters like frequency resonance, input impedance and the radiation pattern, is found in literature, [29],[30]. Analytically and numerical methods for analysis with help of micro strip line theory is used although it is complex and lengthy process, but recently the modeling software like HFSS are used to search for optimum design parameters that achieves max gain, moderate bandwidth and a beam-width that is suitable for sector coverage application. The effect of substrate curvature on the antenna performance is also investigated. One of the methods often used in analysis is the conformable mapping techniques presented by Gupta and Singh in [29], a transformation to an equivalent planar substrate brings the problem in hand back to easier problem.

4.6 Effect of Cylindrical Curvature on Antenna Parameters

It was noticed from simulation that the curvature of the cylinder didn't affect the antenna performance, the resonance frequency is slightly changed while the radiation pattern of the first prototype was unchanged. Apparently that's because the strip radiating edge is aligned to the longitudinal dimension of the cylinder as shown in Fig.4.7. That means the substrate under the printed strip is almost planar, specially that the print strip width is very narrow ($W <<< \lambda$)

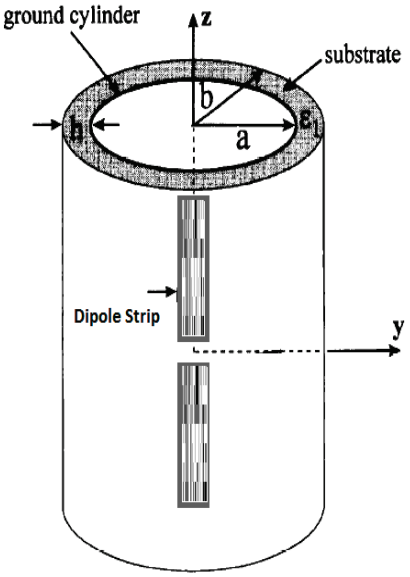

Figure 4.7: Printed dipole strips on cylindrical substrate

4.7 Square Corner Reflector

The objective is to design a CR and to analyze it we will employ the image theory. The finite reflectors are replaced by an array of dipoles with distance (s) from the corner. The corner angle is called the aperture angle α where $\alpha = \pi/n$ and n is any positive integer. The resulting images of the dipole constitute a circular array of 2n element with π radians phase shift of adjacent elements and having same magnitude. Array factor will be derived based on images shown in Fig.4.8

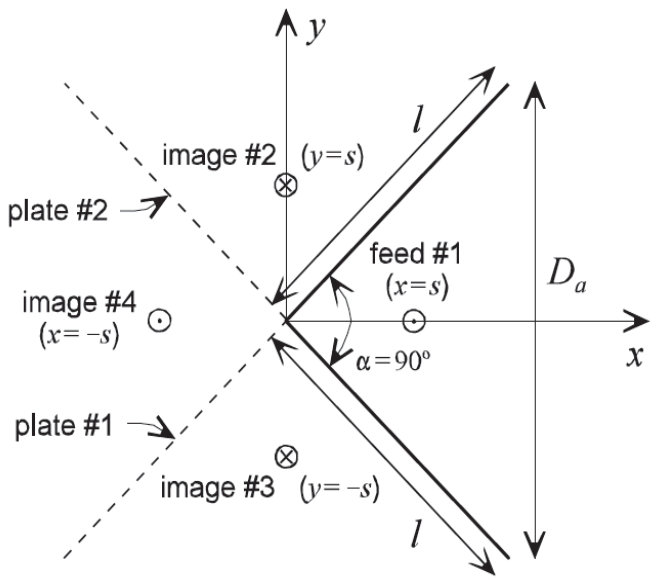

Figure 4.8: 2D representation of the 90 Deg CR with images

For a square corner reflector(SCR) , the angle $\alpha = \pi/2$ depicts that $n = 2$ and hence a circular array of $(2n = 4)$ elements is assumed by image theory. Assume that the number of dipoles $(m = 2n)$ equally spaced around the circumference of the circle with radius (s), as shown in Fig.4.8.

The mathematical derivation of the array factor start with assuming that the

image theory suggests an array that consists of 2 arrays, each has two elements. Considering the first array made of image 1 and image 4, located in the xz plane with current flow in the +z direction, then the array factor can be given by:

$$AF1 = 2 * cos(k * s * sin(\theta)cos(\phi)) \tag{4.8}$$

similarly, for image 2 and image 3, located in the yz plane, and current flow in the -z direction :

$$AF2 = -2 * cos(k * s * sin(\theta)sin(\phi)) \tag{4.9}$$

The total Array Factor for the array of 4 elements is given by:

$$AF = 2 * cos(k * s * sin(\theta)cos(\phi)) - 2 * cos(k * s * sin(\theta)sin(\phi)) \tag{4.10}$$

In the direction of max radiation, the azimuth plane(H-plane), $\theta = \pi/2$ the above equation is reduced to :

$$AF = 2 * cos(k * s * cos(\phi)) - 2 * cos(k * s * sin(\phi)) \tag{4.11}$$

The equations shows that the vertex distance is the main variable that controls the radiation pattern shape. Accordingly, the array factor is found very sensitive to the radiating element vertex distance to the corner. To study the impact of varying the vertex distance (s), a MATLAB code is developed for CR general formula Eq.4.11, and polar plots for the field of the Array Factor is shown in Fig4.9.

The radiation pattern has evolved from single lobe to three then two lobes depending on the distance (s). The initial value used for S was 0.235λ, and as we increase the distance to 0.8λ, two side lobes emerge. Further increase of the distance resulted in a third lobe which builds up until the side lobes vanishes.

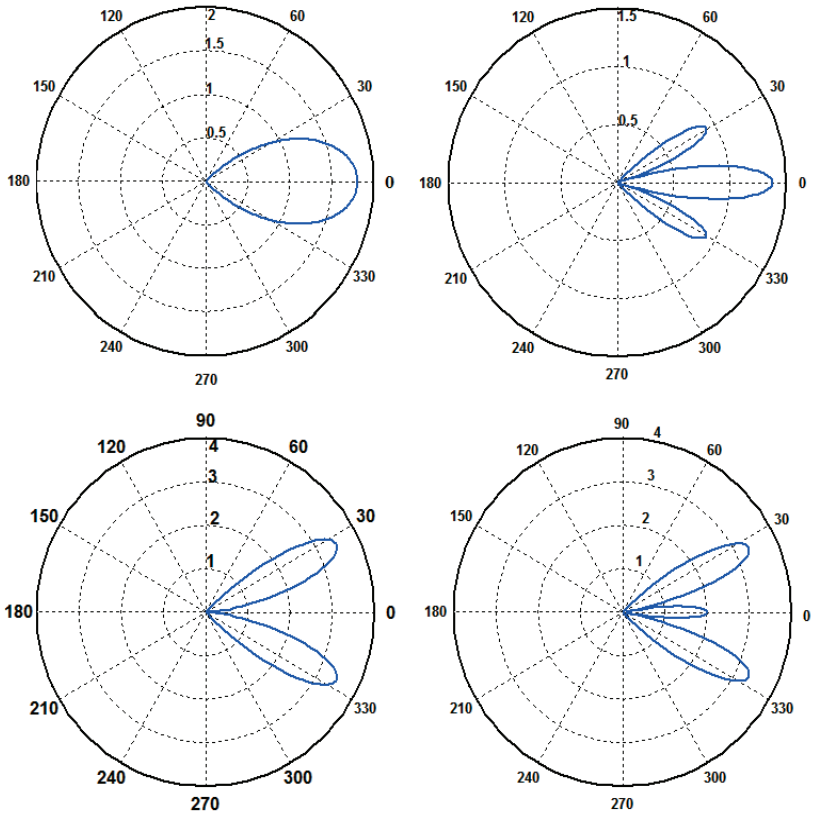

Figure 4.9: CR radiation pattern vs S1 for s1=0.235, 0.8, 1.0, and 1.25 lambda respectively

The SCR increases the gain in most cases to about 12dB compared with the ideal dipole antenna gain which is 2.15dBi. The H plane of the CR antenna is mainly controlled by adjusting the corner angle and distance from the feed to the apex, while the E plane radiation is controlled by staking of antenna feeds in array form. This property of SCR is very essential in beam forming and interference mitiga-

tion. A null can be introduced in the direction of interfere to ensure immunity of the receiver to the adjacent and co channel interference.

To obtain the total antenna radiation intensity; we have to multiply the array factor Eq.4.11 by the dipole pattern, hence :

$$U_{SCR} = (AF)\frac{\eta|I_o|^2}{(2\pi)^2}\{1 - cos\frac{kL}{2}\}^2 \tag{4.12}$$

Also the radiated power of a single dipole is given by Eq.4.13 which dependents on the self resistance R11 of the dipole and R12 the mutual resistance between the images.

$$P_{in} = |I_o|^2\{R_{11} + R_{12}(2s) - 2R_{12}(\sqrt{2}s)\} \tag{4.13}$$

Combining the above equations together we can find an expression for the directive as a function of θ ,

$$D_\theta = \frac{4\pi U_{SCR}}{P_{in}} \tag{4.14}$$

which can be simplified;

$$D_\theta = \frac{2\eta}{(\pi)}\frac{\{cos(ks * cos(\phi)) - cos(ks * sin(\phi))\}\{1 - cos\frac{kL}{2}\}^2}{R_{11} + R_{12}(2s) - 2R_{12}(\sqrt{2}s)} \tag{4.15}$$

4.8 Square Cylindrical Corner Reflector

The squared CCR is a modification on the SCR, with a cylindrical surface added as suggested in [1], and further simplified in [6]. Fig.4.10 shows the schematic

diagram for the proposed modification. Main parameters are the location of the feed R(or vertex distance s), location of the reflecting surface a, thickness of the substrate h, dimensions of the reflecting plate L and W, and the corner angle α.

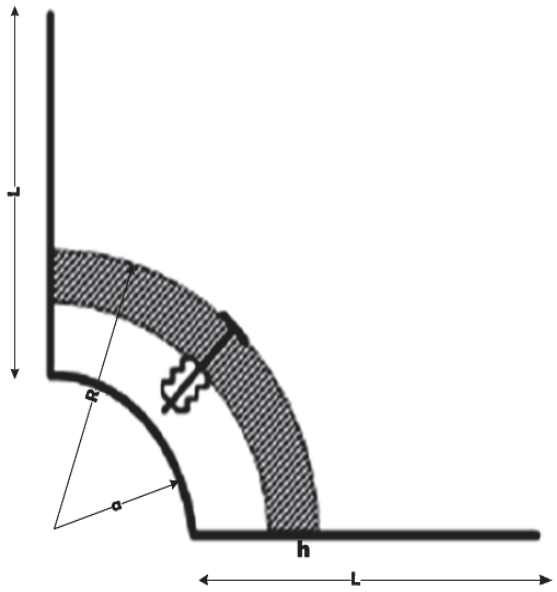

Figure 4.10: CCR with PDA schematic diagram

The side lobe level is controlled by adjusting the vertex distance to the feed (s). The following basic formula for AF in case of square CR is used.

$$AF = 2 * [cos(k * s * cos(\phi) - cos(k * s * sin(\phi)] \tag{4.16}$$

Including of the cylindrical surface results in a second array of images. Using the array factor equation developed for the SCR, the array factor for the first array of images is given by:

$$AF_{inner-array} = 2 * [cos(k(\frac{a^2}{R})cos(\phi) - cos(k(\frac{a^2}{R})sin(\phi)] \tag{4.17}$$

where (a) is the radius of the cylindrical reflecting surface. And the array factor for the second array of images is given by

$$AF_{outer-array} = 2 * [cos(k * R * cos(\phi) - cos(k * R * sin(\phi)] \tag{4.18}$$

where R is the vertex distance of the main feed element.

Different values of (s) are tried, the radiation pattern and the radiation gain is fully controlled by the distance (s). Fig.4.11 shows the effect of the vertex distance on the radiation pattern. The total radiation pattern is shown in Fig.4.12 as a

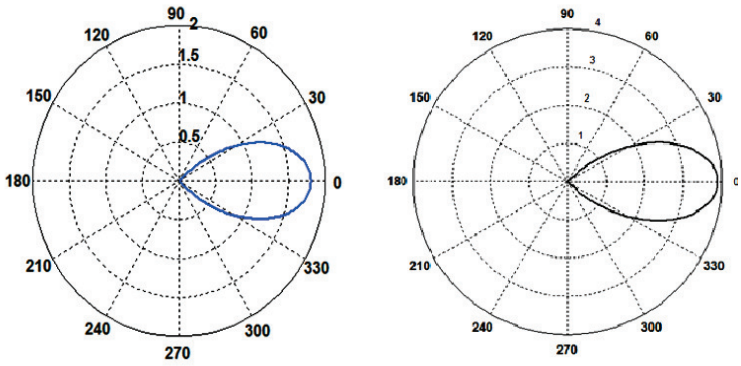

Figure 4.11: Array Factor of the first array(s=0.235lambda) and second array (s=0.45 lamda)

result of combining Eq.4.17 and Eq.4.18. It shows a max radiation at 11.4 dB, and it is the same value we got from the CCR antenna(with printed dipole feed) when the structure is simulated using HFSS.

Although the image theory requires that the reflecting planes should be infinite to ensure that there is no energy radiation in the side of the antenna, but in reality finite dimensions are used in the design and implementation of the corner

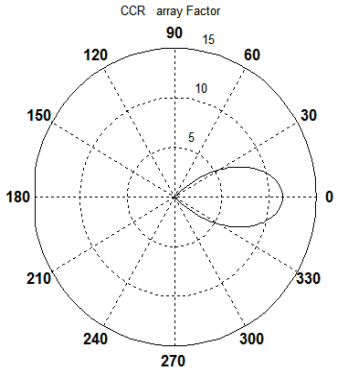

Figure 4.12: Array Factor of the CCR

reflector for UHF frequency application. At low VHF/UHF frequency, Kraus [16] gave general guidelines for the selection of design parameters of the reflecting plats to achieve optimum design. The length of the plate should be at least twice as the vertex distance (s), and the height should be at least 0.6λ. We have chosen one wavelength for both length and width of the reflecting plate. A good approximation of the reflecting plate length can be given by the empirical formula:

$$L_{plate} = \frac{N}{BW\pi} \tag{4.19}$$

where BW is the desired beam width in radians, and N is an integer which is given by $N = 180/\alpha$, and α is the corner angle. So if a SCR (N=2) is used to provide a beam width of 30^o, then the reflecting plate length should be 1.216λ.

CHAPTER 5

SIMULATION AND FABRICATION ANALYSIS

This chapter gives a detailed analysis of the results obtained from simulations carried out using HFSS. Comparisons will be made with reference to the theoretical aspects linked to the simulation and results obtained from the fabrication and lab measurements. Any discrepancies noted will be discussed and commented.

5.1 HFSS vs Other EM solvers

The HFSS V12 will be used in this thesis work as an electromagnetic solver due to its flexibility and easy to use, in addition it is licensed for laboratory used in KFUPM. ANSYS HFSS software is the industry-standard simulation tool for 3D full-wave electromagnetic field simulation based on FEM(Finite Element Method) and is essential for the design of high-frequency and high-speed component design. HFSS offers multiple state-of the-art solver technologies based on either the

proven finite element method or the well-established integral equation method. HFSS solver uses a powerful, automated solution process where it is only required to specify geometry, material properties and the desired output. From there HFSS will automatically generate an appropriate, efficient and accurate mesh for solving the problem using the selected solution technology. Using HFSS we will be able to investigate the antenna radiation patterns, return loss, gain, and many other antenna performance parameters mentioned before. HFSS has shown high computational time in some trials specially when using the Genetic Algorithm option when used to search for optimal performance. The HFSS aborted the simulation or took a very long simulation time in some cases. In average, 15 minutes simulation time is needed on every trial.

5.2 Simulation Results

5.2.1 Proving the Assumption

The concern in this work is whether the printed antenna can be modeled using its cylindrical equivalent wire, suggested by [4], Fig.5.1. To support this assumption the simulation of the CCR using an equivalent cylindrical feed is done Fig.5.2. The radius of the feed wire is $a = 0.25W$ and is equal to 1.25mm, and the results shown a high agreement with the results we got using the printed strip dipole as feed. The simulation results produce an impedance bandwidth of 300MHz around the resonance frequency of 2.45MHz. The VSWR is kept below 1.8, a peak gain is

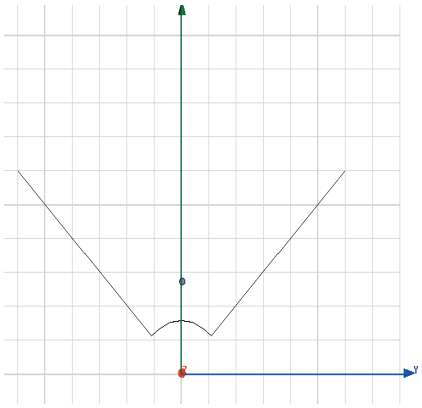

Figure 5.1: prototype-CCR using Wire antenna instead of Printed Dipole

observed at the E plane with a maximum gain of 12dB at $\theta = \pi/2$, with HPBW of 57^o in the H plane, 38^o in the E plane. The F/B ratio is 35dB.

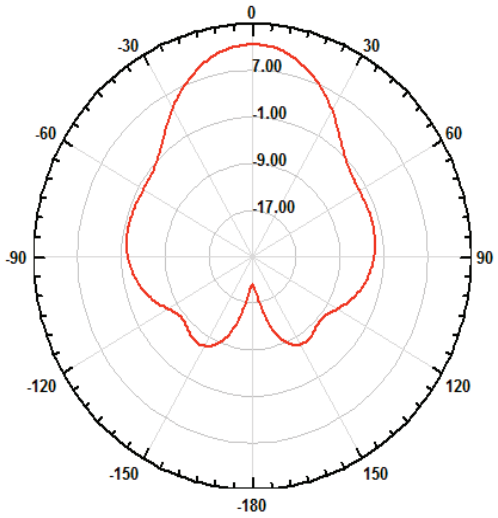

Figure 5.2: Radiation Pattern E plane-CCR using Wire antenna

5.2.2 Shaped Reflector with Printed Antenna Feed

The shaped reflector is constructed by placing a flat reflector under the PDA with two additional inclined CR plates as shown in Fig.5.3 . This type of reflector is similar to the one proposed by [4].

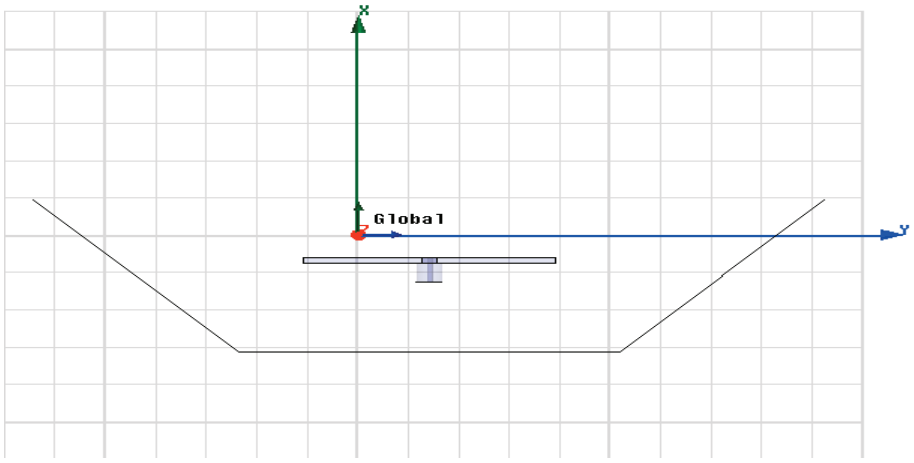

Figure 5.3: Geometry of Shaped reflector with PDA as feed

Compared to the CCR with printed antenna this type is inferior in performance with respect to gain and bandwidth, however its better matching for input impedance. The simulated values are: 10.5dBi, 300MHz, and 50 ohm for above three parameters respectively.

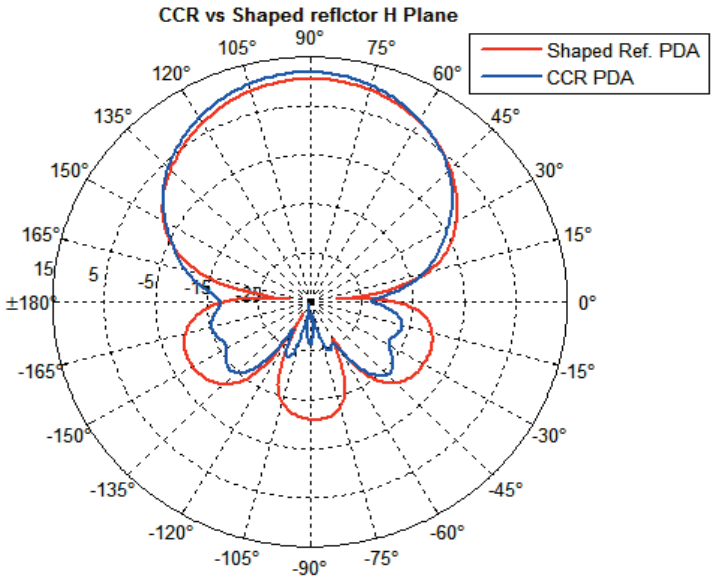

Figure 5.4: H plane radiation pattern for CCR vs Shaped reflector with PDA

Regarding the radiation pattern in the H plane compared with that for the CCR

with PA, Fig.5.4 below shows the two plots. The H plane for CCR is showing better gain and lower side and back-lobes, that is why it is been selected as base for this work.

5.2.3 Proposed CCR with Printed Antenna Feed

As discussed in the methodology earlier, the design has gone through four phases, at which the geometry is simulated and antenna performance parameters are investigated. At the end of this section, a summary table presents the comparative analysis of the final antenna is illustrated.

- Printed Strip Antenna on a Planar substrate . The geometry below is designed and simulated. The design shown in Fig.5.5 is based on research done by [2], [3], [26]. The feeding system is a novel one in our case, where the dipole strips are fed from the center by 50Ω co axial prob. The results show

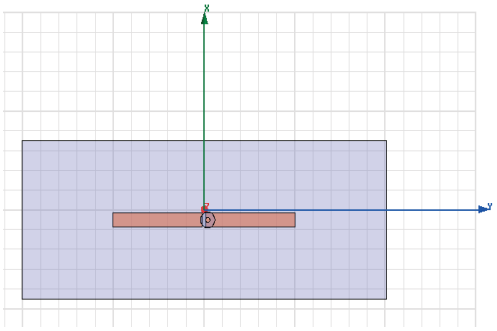

Figure 5.5: Printed Dipole Strips on Planar Substrate

a very good shape for omni directional antenna which resonates at 2.4GHz with 3dB impedance bandwidth of 350Mhz, and VSWR below 1.8. This enables us to use the industrial SMA 50Ω connector for fabrication. The 2D

radiation pattern in the E and H planes shown in Fig.5.6 must agree with the theoretical expected radiation of cylindrical wire dipole placed in free space.

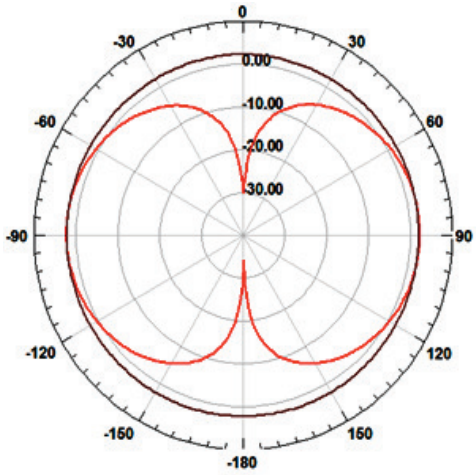

Figure 5.6: PDA on planar substrate- 2D radiation in E and H planes

- The Cylindrical Substrate printed Strip Antenna

  The second phase of the antenna simulation is to design a cylindrical substrate. A right angle cylinder is used with radius R and height L. The radius must be selected carefully since it is going to be considered as the distance between the feed and the corner, in which it has an important influence on the radiation pattern and gain.

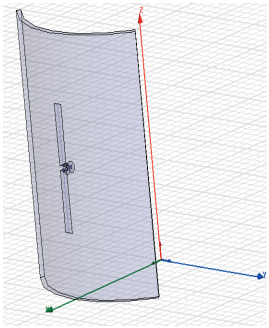

Figure 5.7: Printed Dipole Strips on Quarter Cylindrical Substrate

The parameters are optimized to provide optimum performance of the antenna. The other substrate parameters like: thickness and dielectric constant are kept unchanged. As one can see from Fig.5.8, the simulated radiation patterns are very close to the previous case of planar substrate Fig.**??**. Only a slight shift in resonance frequency has been noticed. The curvature

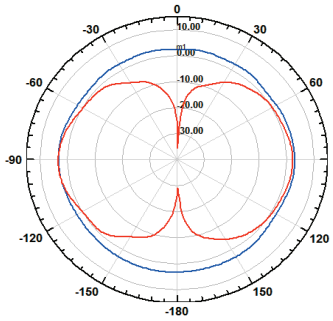

Figure 5.8: 2D Radiation pattern of H and E planes

of the substrate is not changing any of the other radiation parameters. The

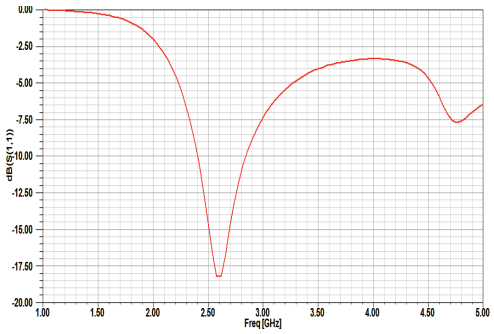

Figure 5.9: The return loss of the PDA, VSWR < 2

return loss figure shows a good agreement at 2.5GHz with VSWR below 2, and 3dB impedance bandwidth of 400MHz

- CCR on a cylindrical substrate

  The final stage is to add the CCR Fig5.10 . The simulation is done and

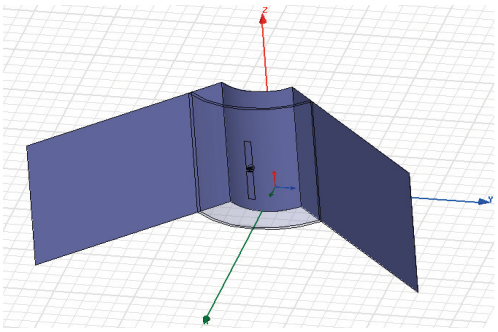

Figure 5.10: CCR with PDA on Quarter Cylindrical Substrate

analyzed. Maximum gain was obtained at 12.4dBi, with HPBW of 33^o, and the 3dB bandwidth of 250MHz at an input impedance of (45-j18)

Observation: increasing the dimensions of the finite reflectors will increase the directivity marginally, at the expense of increasing the size of the antenna.

The 3D radiation pattern of the final prototype is shown in Fig.5.11

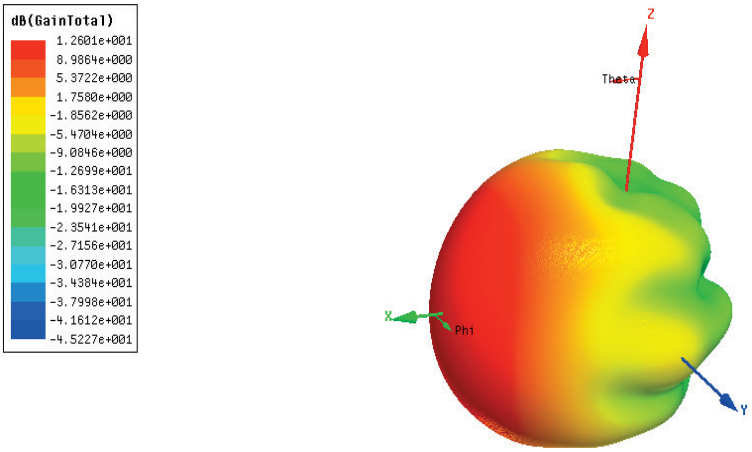

Figure 5.11: The simulated 3D radiation pattern

The E and H plane 2D radiation patterns are shown in Fig.5.12. The HPBW in the H-plane is 57^o and in the E-plane is 33^o, and a front to back ration of 30dB.

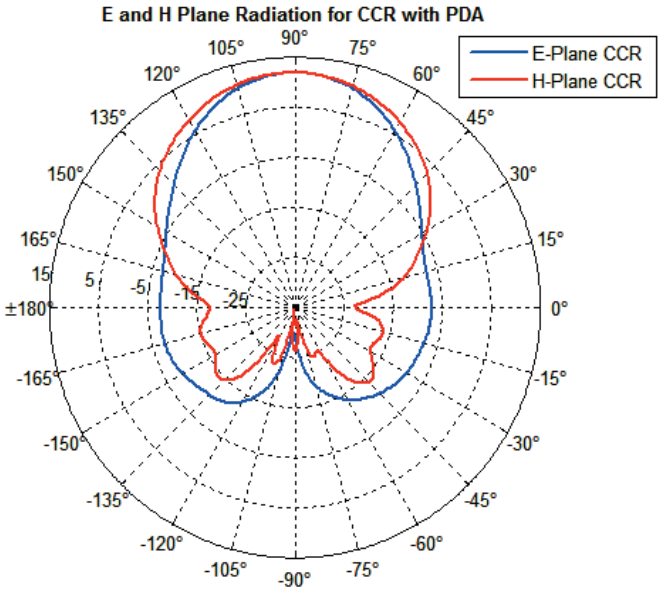

Figure 5.12: The simulated radiation pattern in the E and H planes

The simulated return loss figure is shown in Fig.5.13. The graph is showing a good dip at 2.4Ghz equivalent to a VSWR less than 1.6.

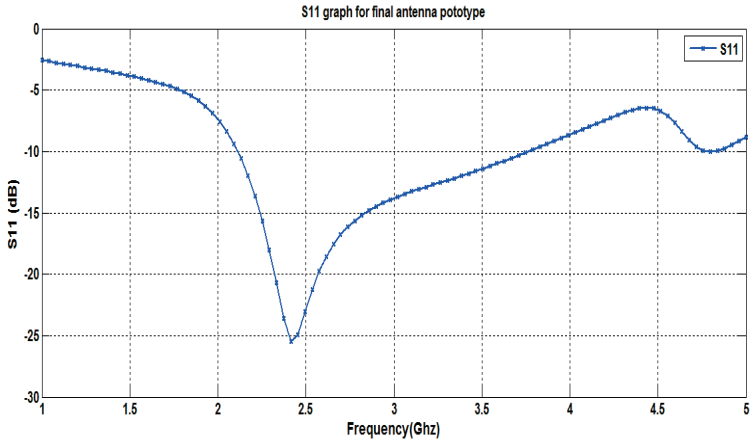

Figure 5.13: The simulated return loss graph for the final CCR

5.3 Optimization processes

Typically a finite corner reflector plates will result in a pattern that is broader than that of the infinite plates investigated theoretically. Therefore, optimization techniques are used to reduce the side lobe level, and prevent energy radiation in an undesirable directions. Below are some techniques found in literature that are used to achieve this objective. We will try to apply it to our proposed antenna and investigate the results.

5.3.1 Off-axis positioning Of Feed

Off axis positioning is used in CR where array of dipoles is used as feed [23]. The antenna is aligned in the co ordinates system such that the radiation pattern will be max in the x direction as shown in Fig.5.11. Off axis positioning is suggested to study the impact of location of the feed on the radiation pattern. At the new location of the feed we have considered an angle of 22.5^o and same vertex distance (s). The E plane radiation pattern is shifted such that the main axis of the beam is directed to -11^o. Fig.5.14 shows the beam direction compared to the on axis feed position.

5.3.2 Radiation Pattern

The two optimization techniques discussed in Ch1 are implemented and the results are presented below. These two techniques aimed at enhancing the H plane radiation pattern to increase the directivity and reduce the side lobe level. In

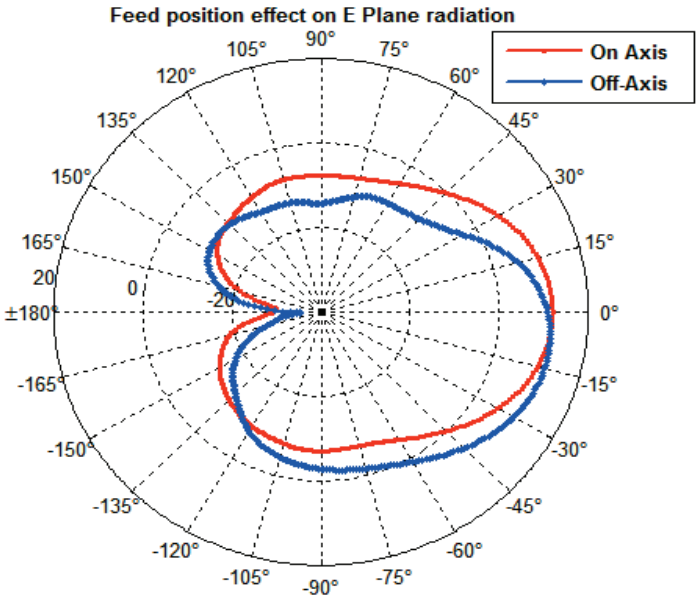

Figure 5.14: Optimized CCR prototype- Triple folded

addition a simple structure and antenna parameters are kept unchanged. Fig. 5.15 and Fig. 5.16 show the modified antenna and Fig.5.17 shows the simulation results using HFSS in the H plane.

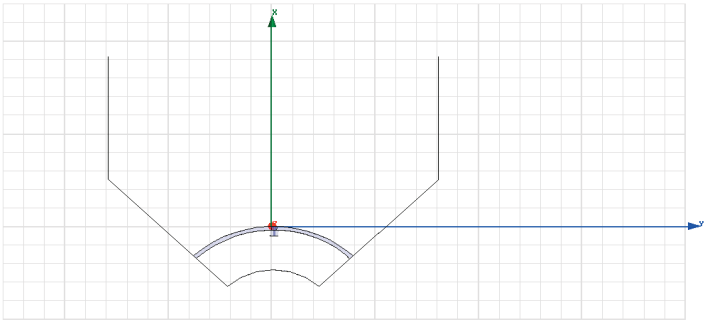

Figure 5.15: Optimized CCR prototype- Triple folded

In both cases the antenna is optimized to give optimum performance, using HFSS Genetic Algorithm to search for the optimum dimension of the reflector planes. The side lobe level and radiation pattern in the H plane are influenced by the position and width of the metallic strips.

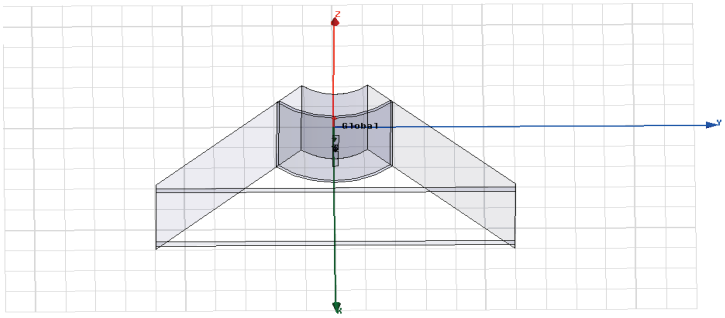

Figure 5.16: Optimized CCR prototype-adding strip scatters

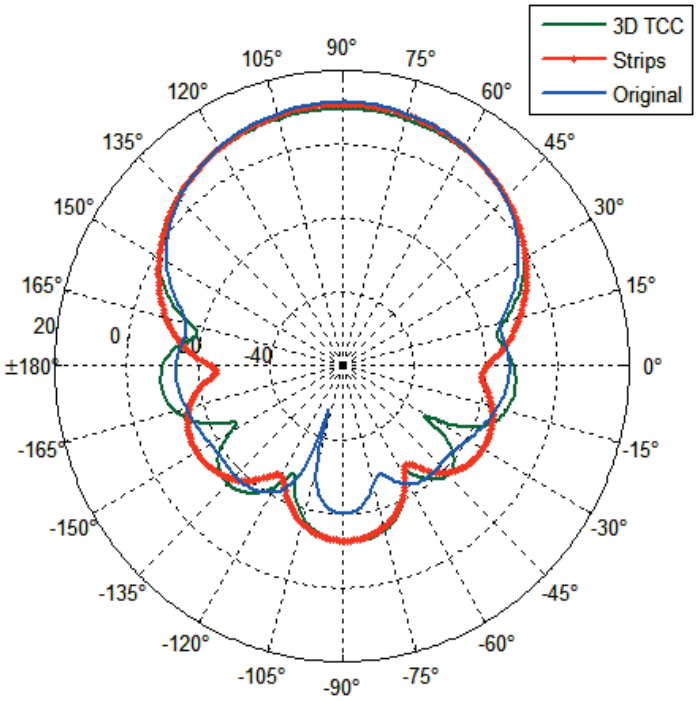

Figure 5.17: Optimization processes on Conventional CCR

Fig. 5.17 shows that the case of 3 dimensional triple-cylindrical corner reflector [10] did not improve the side lobe level, while the case with the metallic scatters [9] did enhancement in the side lobe level compared to the original CCR.

As part of the optimization process we have also tried to increase the dimension of the CR. The height and length of the reflecting planes are increased twice and four times, respectively. The directivity and gain are marginally increased to a limit

of an additional 2dB. This approach can be useful if we don't have a constrain on the allowed space for the antenna since the size and cost will be much higher than the originally suggested antenna dimensions.

The other antenna characteristics results from the optimization techniques are unchanged, the 3dB impedance bandwidth, VSWR, and the return loss input impedance) are all unchanged. This make the above suggested crteria a good solutions if more directivity or gain are needed to meet certain design criteria.

5.3.3 Broadband Antenna

In order to make the antenna bandwidth broader, one way is to add parasitic elements to the printed dipole. The coupling between the dipole and the parasitic strips produce radiation that enhances the radiation pattern and bandwidth, Fig.5.18 shows the HFSS prototype.

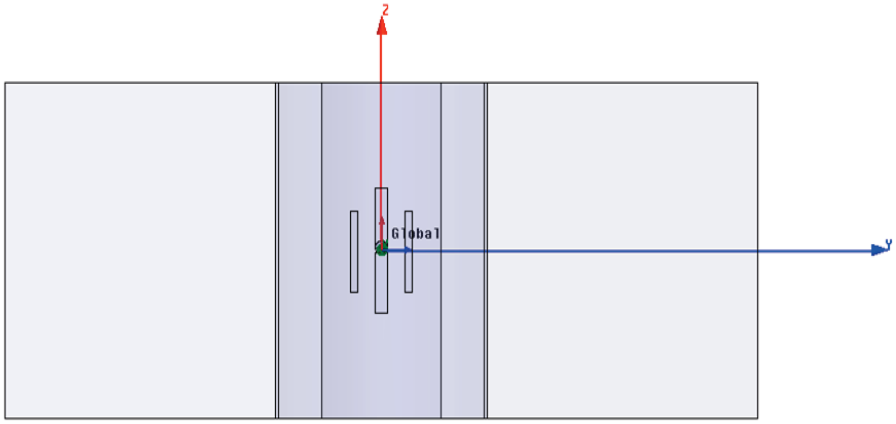

Figure 5.18: Front view of the antenna with addition of 2 parasitic elements

The broadband antenna dimensions are optimized to provide a wide 3dB bandwidth as shown in Fig. 5.19. The 3dB impedance bandwidth is around 1.3GHz

covering a multiple 3GPP frequency bands used in Mobile Industry beside the WiFi as a prime application to this thesis work.

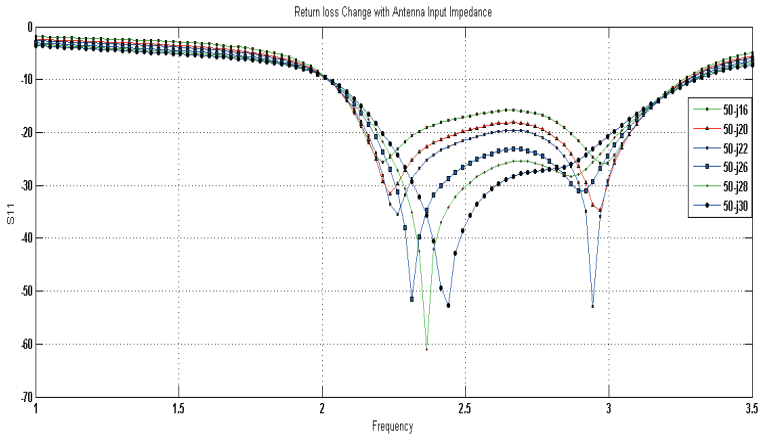

Figure 5.19: S11 vs Input Imp. Optimization processes on BroadBand

Broadband antenna is characterized by two main factors: wide bandwidth,and the radiation pattern. The antenna radiation in one plane must be the same at any frequency within the bandwidth range. Fig.5.20 shows that this condition is satisfied in our case , in addition to a small increase in directivity .

On the band 2.6GHz used for LTE TDD; the antenna has shown a very good results for the E plane radiation where the side lobs are reduced and the total directivity is increased to 14.5dB compared to our original antenna.

5.4 Fabrication And Lab Testing

5.4.1 Fabrication of CCR and The Printed Antenna

The Printed strip antenna was printed on a semi rigid Roger PCB Duroid TM, and using LPKF printing board plotter machine(S63)for Milling and Drilling of

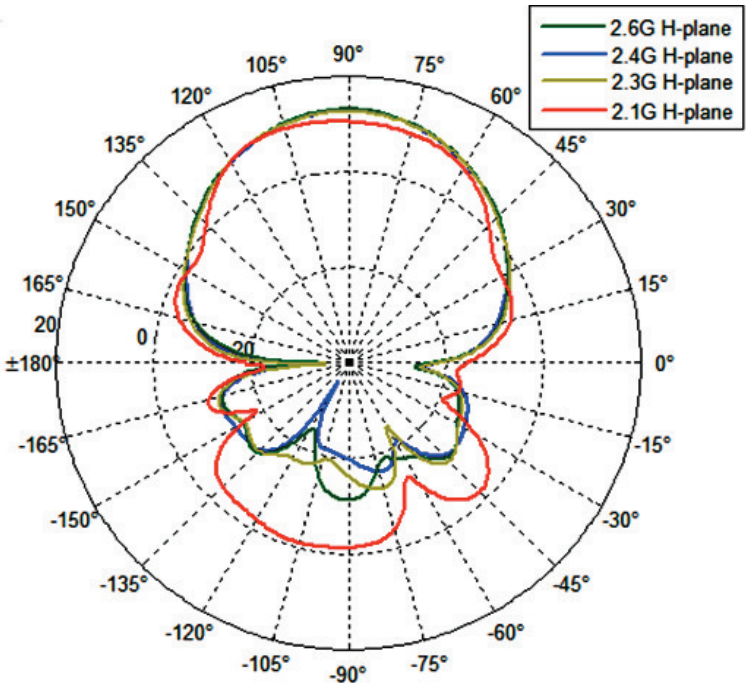

Figure 5.20: E Palne Radiation pattern for different Frequency bands

the prototype. The drilling of the PCB is needed to be able to solder the SMA 3.5mm co axial connector as center feed. The result PCB with printed dipole antenna is treated with heat and pressure to allow a curvature of the quarter cylindrical shape to obtain designed curvature. Further step is taken to prepare the CCR reflecting surfaces, cutting and welding using designed dimensions. The final prototype is shown in the fig 5.21.

5.4.2 Testing Results- S11 And BW

The proposed antenna is fabricated locally at the lab and tested using the Agilent vector network analyzer E5071C(ENA series) to measure the return loss scattering parameter. The measured S11 is showing a very good results with 3dB impedance bandwidth of 310MHz, which has good agreement with the simulation results.

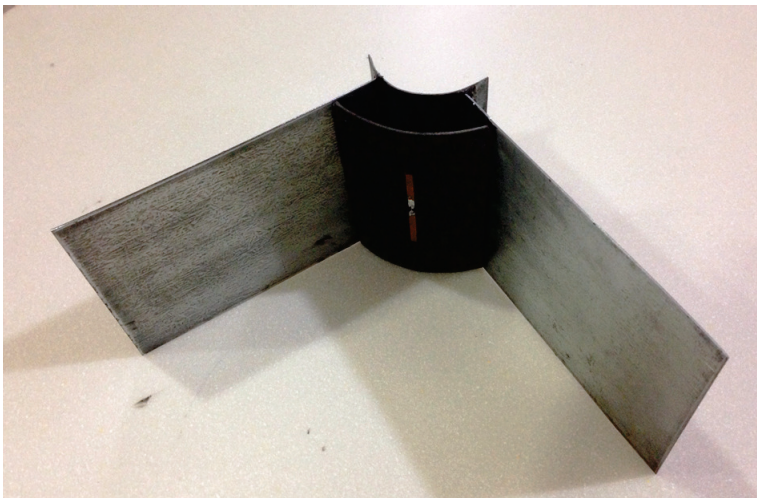

Figure 5.21: CCR with strip dipole feed fabricated prototype.

The measurement was repeated for two different values of CCR radii versus the vertex distance R. The obtained results shown in Fig.5.22 has some dependency of the resonance frequency due to the location of the feed with respect to reflecting surfaces. Similar observation was mentioned by [4]. There is a negative effect on frequency resonance when the antenna is placed close to perfectly conductive reflecting surfaces. There is some distortion in the graph of S11 due to VNA calibration.

5.4.3 Testing Results- E And H Radiation Pattern

Antenna radiation characteristics are normally measured in the anechoic chamber. The anechoic chamber shown in Fig.5.23 is a special room that is used to measure antenna radiation patterns. The chamber itself is an electrically sealed metal enclosure designed to prevent external signals from penetrating and interfering to the inside chamber and corrupting the measurements. The internal walls of the chamber are lined with special cone-shaped carbon perfectly designed pyramidal

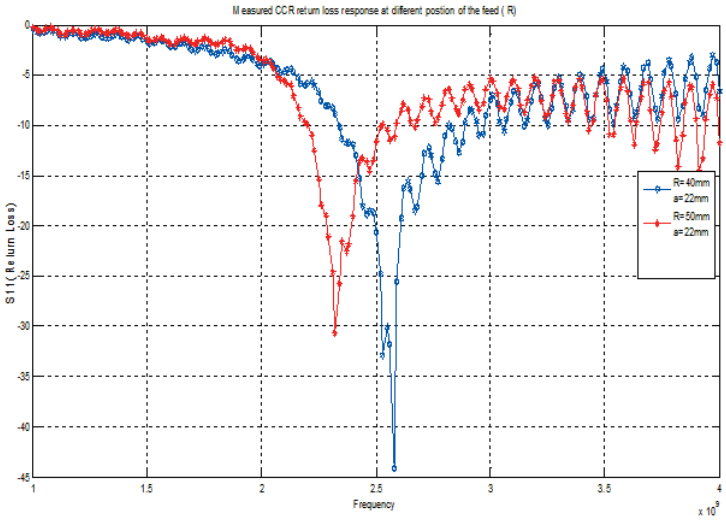

Figure 5.22: Measured S11 Retrun Loss parameter for the fabricated antenna.

electromagnetic absorbing material. The shield characteristics of the chamber is preferred to be as high as possible($> 90dB$) to ensure isolation of out side environmental conditions. From an electromagnetic perspective, the inside of the chamber is indistinguishable from a free-space environment because the walls do not reflect or echo any power back into the room (hence the name anechoic chamber)shown in Fig5.23.

A non isotropic antenna radiates energy in specific direction more than other di-

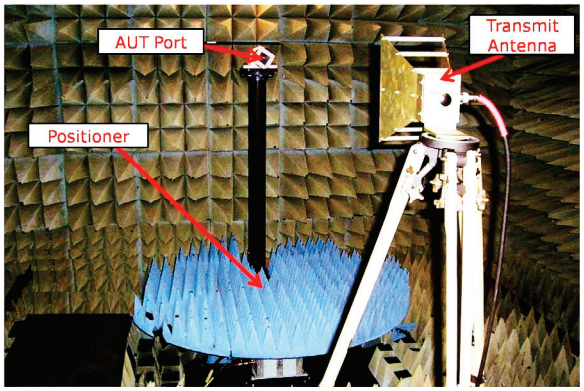

Figure 5.23: Anechoic Chamber Setup and Lab equipment arrangement.

rections, hence the measurement of power as a function of angle gives the radiation

pattern. Many antenna parameters associated with the radiation can be tested using the anechoic chamber : the polarity (horizontal and/or vertical, circular, etc.) is measured , directivity, gain, side lobe level are other related parameters. Radiation pattern is normally given in terms of power rather than field or voltage and most often is given in decibels rather than linear terms.

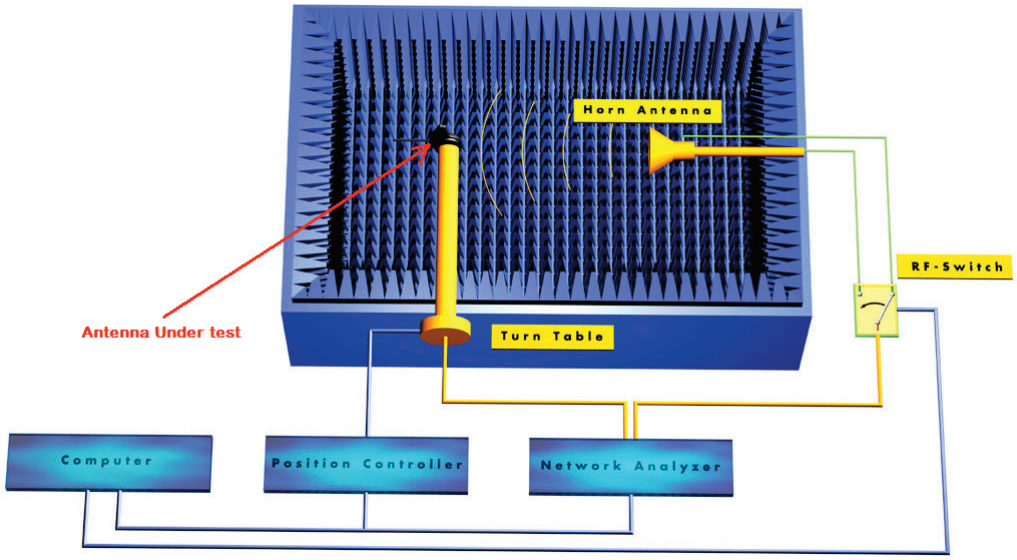

Figure 5.24: Radiation pattern measurement in the Anechoic Chamber.

To measure the radiation pattern characteristics of an antenna the anechoic chamber is setup like in Fig.5.24. A calibrated horn antenna is usually used as a source of radiation and the antenna under test is to receive the radiation. Fig. 5.25. The E and H plane measured pattern is showing a good front to back ratio of 13dB which reflects the directivity of the antenna in the intended radiation direction. From the measured data the efficiency of the antenna has been degraded and that is probably due to matching characteristics during the test. This problem can be easily overcome by sliding the printed dipole substrate and choosing

different vertex distance. It was shown before, that the vertix distance has a big influence on the matching characteristics of the antenna input impedance.

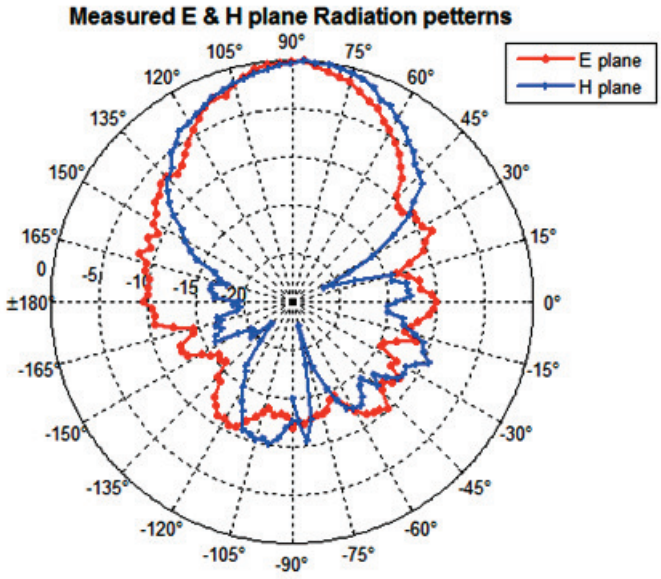

Figure 5.25: Measured H Plane Radiation pattern for the fabricated antenna.

Fig5.26, shows the E plane measured radiation pattern, compared with the simulated one, and they are found in a good agreement. The HPBW is 56^o with F/B ratio of around 12dB.

5.5 Antenna testing at Field - Actual Case Study

After successfully completing the simulations and lab measurements of the radiation pattern and the return loss for the designed antenna, we have taken the antenna to the field where real world implementation is proposed. We have selected one indoor coverage solution for 2G/3G/LTE which is implemented by one

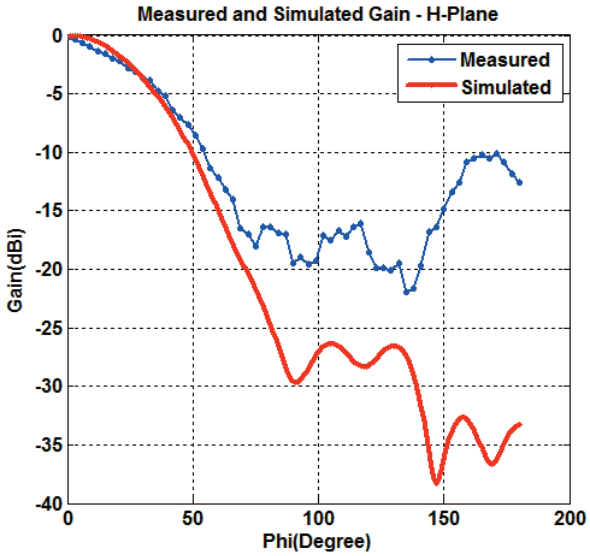

Figure 5.26: Measured E Plane Radiation pattern for the fabricated antenna.

Mobile services provider in KSA , city of Khubar. The implemented current solution in Dhahran Mall was investigated to check how we can integrate our proposed antenna. The following comments were found which shows that the current model suffers from few design short comes that could be overcome by using directional antenna similar to the proposed one in this thesis.

- The current design supports only 2G/3G , no provision for LTE or WiFi. Therefore, future expansion will require new design, new installation, and new lease agreement with site owner.

- The current design uses omni antenna hence there are large number of antennas needed and lot of power splitters and combiners, which leads to large power losses and limited coverage.

- Large number of antenna means many lease agreement with owner which scales to higher rent fees and high CAPEX to be invested.

- Having many antennas and feeders, spliters, combiners results in a complex and difficult to maintain system, high OPEX.

The key solution for above drawbacks is using of directional antenna with wide-band operation that covers different mobile broad band frequencies. This is suggested by using our CCR antenna with printed dipole.

To prove that our concept is applicable we have used a special software in simulating the coverage inside and out side the buildings. The parameter used are shown in the table 5.1 :

Table 5.1: Field simulation Parametrs

Designed Frequency	2.4 GHz
TX power	0.25 Watt
Omni Antenna Gain	2.15 dBi
Directional Antenna Gain	12.5 dBi

Fig5.27 shows the implemented design using Omni directional antenna at transmission power typically at 0.25W, coverage gaps are clearly shown in red color, due to nature of omni antenna radiation.

The same simulation parameters above are used but using the proposed directional antenna , and we clearly see a continuous coverage, more importantly less number of antennas are needed to cover the same area. Fig5.28 shows the results.

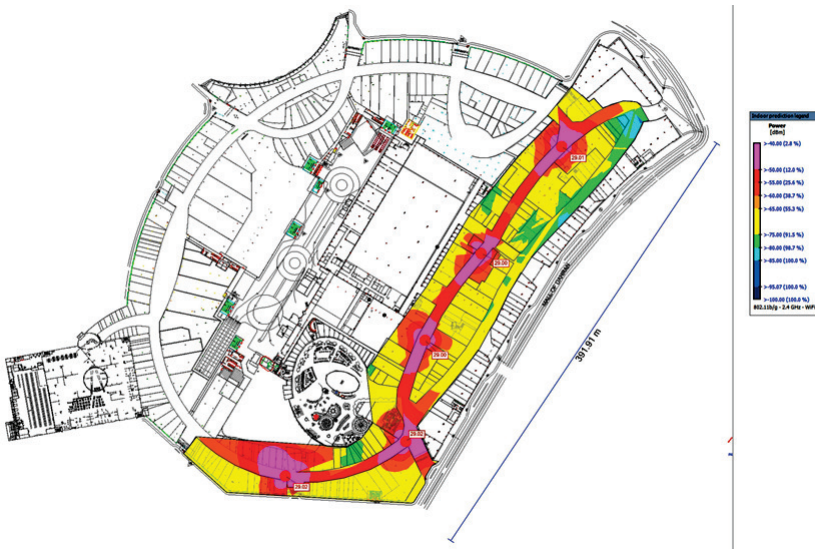

Figure 5.27: Simulated Radiation pattern with 0.25W 2.15dB for the field OMNI antenna.

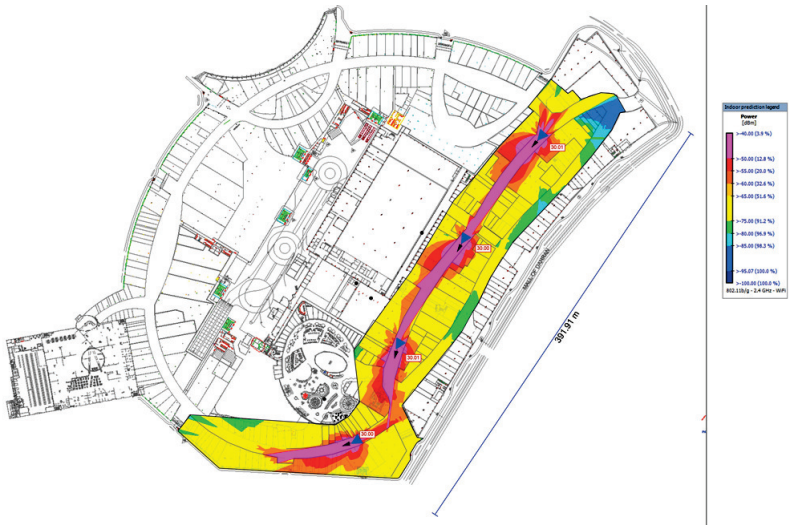

Figure 5.28: Simulated Radiation pattern with 0.25W 12.5dB for the proposed directional antenna.

CHAPTER 6

CONCLUSIONS AND FUTURE WORK

6.1 Summary

Cylindrical Corner reflected fed by printed strip dipole is studied here. Designed, simulated using the HFSS, implementation and experimental measurements are carried out for the proposed antenna. The antenna is designed for the WiFi frequency bands and extended to be used for other 3GPP applications. The effects of various antenna parameters on the radiation pattern and return loss are investigated through out our study. Various designs for printed dipole and CCR were investigated and finally we have selected specific dimensions and dielectric material for optimal performance. The design of the proposed antenna evolved from simple planar printed antenna on a thin substrate to a printed strip antenna on a cylindrical substrate with CCR through four steps. Antenna characteristics

like radiation pattern in the elevation and azimuth planes, return loss, input impedance, and 3dB impedance bandwidth are analyzed and investigated. Effect of the cylindrical curvature on the resonance frequency is studied and found to be minimal. A design modification to increase directivity and broaden the bandwidth of antenna was also addressed, and has shown very good improvement on the antenna performance. We have shown that the proposed antenna exhibits high side lobes that can be reduced by increasing the length and width of the reflecting plates, thats at the expense of the antenna size.

Most optimal radiation patterns are obtained for cylindrical reflecting surface radius 0.35λ and a cylindrical substrate radius 0.6λ. The dipole is typically half wave length, and CCR plates are 1.5λ and 1λ for length and height. The result shows that the resonant frequency is not negatively affected by the cylindrical curvature however the radiation patterns are significantly affected as per the Image Theory and Circular Array Theory. The radiation pattern in the azimuthal direction is strongly dependent on the cylinder radius and the length of the plates, the elevation direction it is independent on these factors.

6.2 Conclusions And Future work

The research work presented here aims at designing a novel directional antenna based on CCR and fed by printed dipole for the WiFi frequency range. The antenna parameters were optimized to provide a broadband range of frequencies that covers other 3GPP wireless communication standards. Providing the necessary

equations for the design of printed dipole antenna. The simulation and fabrication process of a the CCR antenna is presented and many interesting results are illustrated. There are few techniques to enhance the antenna characteristics specially the bandwidth.

The addition of parasitic elements beside the radiating element is used to achieve such target. Consequently, the resonant frequency of the coupled elements is slightly different from the driven element, but the bandwidth of the entire antenna may be increased. The antenna was kept very simple and low cost, while providing a highly directive radiation characteristics with broaden bandwidth. Printed antennas are in general very attractive option as feed element when it is required to have low cost and simple design. It is selected as a feed system for the proposed antenna due to some other advantages in comparison with the conventional radiators. During the design and fabrication of the CCR, few challenges were observed that need further research. Topics that can be explored or expanded following this thesis are listed as follows:

- Design of MIMO system using the proposed antenna.
- Apply beam scanning techniques.
- Reducing Losses / increasing efficiency
- Improving feed networks, and input matching.
- Size reduction techniques.

REFERENCES

[1] H. M. ELkamchouchi, "Cylindrical and Three-Dimensional Corner Reflector Antennas," *IEEE Transactions on Antennas and Propagation,*, vol. 31, no. 3, pp. 451–455, 1983.

[2] M. Jamaluddin, M. Rahim, M. Aziz, and a. Asrokin, "Microstrip Dipole Antenna Analysis with Different Width and Length at 2.4 GHz," *2005 Asia-Pacific Conference on Applied Electromagnetics*, pp. 41–44, 2005.

[3] A. Asrokin and M. H. Jamaluddin, "Microstri Dipole Antenna For WLAN Aplication," *Computers, Communications, & Signal Processing with Special Track on Biomedical Engineering, 2005. CCSP 2005. 1st International Conference*, pp. 30–33, 2005.

[4] F. Tefiku, "Broadband sector zone base station antennas, Antennas and Propagation for Wireless Communications, 1998. 1998 IEEE-APS Conference," pp. 109–112, 1998.

[5] J. D. T. H.P.Neff, "The uesign of the Corner-Reflector Antenna," vol. 19, no. 604, pp. 293–296, 1959.

[6] M. K. Abdelazeez, "Cylindrical corner reflector aantenna," pp. 496–499, 1987.

[7] M. Khodier and M. Al-Aqeel, "Linear And Circular Array Optimization:A Study using Practice Swarm Intelligence," *Progress In Electromagnetics Research B*, vol. 15, pp. 347–373, 2009.

[8] V. P. Joseph and K. T. Mathew, "A Novel Corner Reflector Antenna," *Microwave and Optical Technology Letters*, vol. 30, no. 6, pp. 403–404, 2001.

[9] A. Harmouch, C. El Moucary, M. Ziade, J. Finianos, C. Akkari, and S. Ayoub, "Enhancement of directional characteristics of corner reflector antennas using metallic scatters," *2012 19th International Conference on Telecommunications (ICT)*, no. Ict, pp. 1–4, Apr. 2012.

[10] K. T. Mathew, J. Jacob, S. Mathew, and U. Raveendranath, "Triple corner reflector antenna and its performance in H-plane," vol. 32, no. 16, p. 1996, 1996.

[11] C. Balanis, "Antenna theory: A Review," *Proceedings of the IEEE*, vol. 80, no. 1, pp. 7–23, 1992. [Online]. Available: http://ieeexplore.ieee.org/lpdocs/epic03/wrapper.htm?arnumber=119564

[12] W. L. Stutzman, *Antenna Theory and Design*, 1981.

[13] C. A. Balanis, *Advanced Engineering Electromagnetics*. Wiley, 1989, vol. 52, no. 1.

[14] IEEE, *"IEEE Standard Definitions of Terms for Antennas"*, Feb 1983.

[15] D. M. Pozar, *Microwave Engineering*, B. Zobrist, P. Kulek, and G. Aiello, Eds. Wiley, 2005, vol. Third.

[16] J. D. Kraust, "The Corner-Reflector Antenna," vol. 27, no. 1, pp. 19–23, 1940.

[17] C.-H. L. Dau-Chyrh Chang, "Prime Feed Reflector Antenna for Applications of Site Survey," *Proceeding Of ISAP2005, Seoul, Korea*, pp. 237–240, 2005.

[18] A. Nesic, Z. Mici'c, S. Jovanovi'c, I. Radnovi'c, and D. Nešić, "Millimeter Wave Corner Reflector Antenna Array."

[19] *http://www.radio-electronics.com/info/wireless/wi-fi/80211-channels-number-frequencies-bandwidth.php*.

[20] *http://3gpp.org/specifications/67-releases*.

[21] Naoki Inagaki, "Three-Dimensional Corner Reflector Antenna," pp. 580–582, 1974.

[22] S. Ali-hossain, B. S. Sharif, and G. Chester, "Improved Corner Reflector Anatenna Performnce By Using Cylindrical Reflector," 2002.

[23] H. A. Ragheb, "Radiation Characteristics of the Corner Array," pp. INT. J. Electronics, Vol. 60, No. 2, p229–p238, 1986.

[24] T. D. Dimousios, S. A. Mitilineos, S. C. Panagiotou, and C. N. Capsalis, "Design of a Corner-Reflector Reactively Controlled Antenna for Maximum Directivity and Multiple Beam Forming at 2.4 GHz," pp. 1132–1139, 2011.

[25] J. A. Romo, I. F. Anitzine, and J. Garate, "Optimized Design of Cylindrical Corner Reflectors for Applications on TV Broadband Antennas," vol. 26, pp. 937–944, 2011.

[26] J.-m. Floc, J.-m. Denoual, and K. Sallem, "Design of Printed Dipole with Reflector and Multi Directors," no. November, pp. 421–424, 2009.

[27] F. Tefiku and C. A. Grimes, "Design of broad-band and dual-band antennas comprised of series-fed printed-strip dipole pairs," *Antennas and Propagation, IEEE Transactions on*, vol. 48, no. 6, pp. 895–900, 2000.

[28] M. Strom, "Design of a broadband antenna element for LTE base station antennas," 2009.

[29] S. D. Gupta, A. Singh, C. Engineering, and A. Technologies, "Design and Performance Analysis of Cylindrical Microstrip Antenna and Array using Conformal Mapping Technique," vol. 02, no. 03, pp. 166–180, 2011.

[30] R. Sreekrishna and G. R. Kadambi, "Design And Development of a Compact Wideband Conformal Antenna for Wireless Applications," *SASTech*, vol. Volume 10, no. Issue 1, pp. pp36–42.

[31] D. M. Pozar, "Microstrip Antennas," vol. 80, no. 1, 1992.

[32] C. Votis, "Geometry Aspects and Experimental Results of a Printed Dipole Antenna," *Int'l J. of Communications, Network and System Sciences*, vol. 03, no. 02, pp. 204–207, 2010.

[33] B. Ahmed, I. Saleem, H. Zahra, H. Khurshid, and S. M. Abbas, "Analytical Study on Effects of Substrate Properties on the Performance of Microstrip Patch Antenna," vol. 5, no. 4, pp. 113–122, 2012.

[34] C. Y. Chu, *Printed Dipole Antenna Design For Wireless Communications*, 2005, no. July.

Vitae

- Name: Eqab Fahad AbdulRahim Khleif
- Nationality: Palestinian
- Date of Birth: 1975
- Email: *ekhlaif75@gmail.com*
- Permanent Address: Khubar - KSA
- I have received my Bachelor degree from Applied Science University in Amman-Jordan 1998, I am currently working toward mys master degree of Electrical Engineering at King Fahd University for Petroleum and Minerals. I have around 15 years of industrial experience in the field of 2G/3G/LTE backhaul systems planning and design in different regional mobile Operators. My main topics of interest are antennas and propagation, smart antennas , fiber optics communication, microwave systems, and wireless personal communication. I have participated in Advanced Electromagnetic Symposium Held March 2013 in UAE presenting this thesis work, and have submitted a paper to ACES journal for publication. I am currently working on a new publication in IEEE Journal Review.